THE IMPACT OF EXPERIMENTAL DESIGNS & SYSTEM SLOPPINESS ON THE PERSONALISATION PROCESS: A CARDIOVASCULAR PERSPECTIVE

Harry Saxton
School of Computer Science
Insigneo Institute for in silico Medicine
University of Sheffield
Sheffield, United Kingdom
h.saxton@sheffield.ac.uk

Daniel J. Taylor
NIHR Sheffield Biomedical Research Centre
Insigneo Institute for in silico Medicine
University of Sheffield
Sheffield, United Kingdom

Grace Faulkner
NIHR Sheffield Biomedical Research Centre
University of Sheffield
Sheffield, United Kingdom

Ian Halliday
NIHR Sheffield Biomedical Research Centre
University of Sheffield
Sheffield, United Kingdom

Tom Newman
Department of Cardiology
NIHR Sheffield Biomedical Research Centre
University of Sheffield
Sheffield, United Kingdom

Torsten Schenkel
Department of Engineering and Mathematics
Sheffield Hallam University
Sheffield, United Kingdom

Paul D. Morris
Sheffield Teaching Hospitals NHS Foundation Trust
University of Sheffield
Sheffield, United Kingdom

Richard H. Clayton
School of Computer Science
Insigneo Institute for in silico Medicine
University of Sheffield
Sheffield, United Kingdom

Xu Xu
Insigneo Institute for in silico Medicine
University of Sheffield
Sheffield, United Kingdom

December 5, 2024

ABSTRACT

To employ a reduced-order cardiovascular model as a digital twin for personalised medicine, it is essential to understand how uncertainties in the model's input parameters affect its outputs. The aim is to identify a set of input parameters that can serve as clinical biomarkers, providing insight into a patient's physiological state. Given the challenge of finding useful clinical data, careful consideration must be given to the experimental design used to acquire patient-specific input parameters. In this paper, we conduct the first quantification of a cardiovascular system's sloppiness to elucidate the structure of the input parameter space. By utilising Sobol indices and examining various synthetic cardiovascular measures with increasing invasiveness, we uncover how the personalisation process and the cardiovascular system's sloppiness are contingent upon the chosen experimental design. Our findings reveal that continuous clinical measures induce system sloppiness and increase the number of

personalisable biomarkers, whereas discrete clinical measurements produce a non-sloppy system with a reduced number of biomarkers. This study underscores the necessity for careful consideration of available clinical data as differing measurement sets can significantly impact model personalisation.

Keywords Cardiovascular Modelling · Personalised Medicine · Digital Twins · Sensitivity Analysis · Parameter Identifiability · Sloppy Systems

Author Summary

In personalised medicine, computational models that replicate physical systems — are becoming vital tools for understanding and predicting individual health. Our study explores cardiovascular models, which simulate heart and circulatory functions from which clinical metrics may be derived. These models aim to provide personalised insights into heart health and treatment planning.

A key challenge in building these models is addressing "sloppiness," a property which provides vital insight into the response surface structure for which one calibrates a model searching for a global minimum point, a position in parameter space which best represents a patients cardiovascular health. In order to personalise a model different types of clinical metrics must be available for a model response to be compared to.

We examined how different types of clinical data — ranging from simple discrete blood pressure readings to detailed invasive continuous waveform data — impact model sloppiness and the number of personalisable biomarkers. Our results show that continuous measurements increase the number of personalisable biomarkers but make the personalisation process more complex through increased sloppiness. In contrast, simpler discrete measurements reduce model sloppiness simplifying the personalisation process but yield fewer personalisable biomarkers. By analysing the impact of experimental designs on the personalisation process, our work offers practical insights into improving the reliability of cardiovascular digital twins, supporting their adoption in personalised medicine.

1 Introduction

The concept of digital twin (DT) originates in the 1960s with NASA creating a virtual representation in the Apollo 13 moon exploration mission. There are now many definitions of DT and one comprehensive definition is "a set of virtual information constructs that mimics the structure, context and behaviour of an individual or unique physical asset, which is dynamically updated with data from its physical twin throughout its life-cycle and that ultimately informs decisions that realise value" [1]. In the realm of medicine, the potential of a DT is profound, particularly in enhancing patient care and outcomes. In the context of healthcare, a regularly updated digital representation of an individual's anatomy, physiology or diseases holds immense promise. It could empower healthcare professionals to simulate and predict a patient's disease trajectory enabling intervention and treatment to be delivered in a timely and effective way [2].

Notably, in cardiology, the adoption of heart and circulatory DTs has gradually gained momentum and trust within the clinical community, evidenced by several proof-of-concept studies [3, 4, 5]. Traditionally, clinical diagnosis and patient trajectories in cardiology rely heavily on a clinician's expertise and population-based averages [6]. However, the emergence of DTs in cardiology signifies a shift towards a more personalised approach. These DTs integrate mechanistic (physics-based) models, grounded in physiological understanding of the heart, human circulation, and related physiological processes, with dynamic clinical data collected over time or immediate data available in a clinical setting [7]. This integration enables the DT tool to provide tailored predictions and assist in clinical diagnosis, catering for the unique characteristics of each patient. Virtual representations of a patient's full cardiovascular health in differing states are referred to as their "physiological envelope" [8].

Clearly, the choice of mechanistic model utilised for a cardiovascular DT is vital to ensure the correct set of physiological relevance while also maintaining some set of clinical interpretability. Lumped parameter models (LPM) offer a unique ability to examine both cardiac function and global haemodynamics. LPM provide a simple approach in which all the main characteristics of the blood flow (i.e. blood pressures, flows and volumes) are captured. Typically, an LPM is constructed of a heart chamber (acting as a blood pump), a presentation of the mechanical nature of heart valves and a series of elements representing the various vascular networks in which blood can be transported through the body. This class of model is usually represented as a system of differential algebraic equations; the size of which depends on the complexity of the system investigated (full body circulation or anatomically detailed models of specific vessels) [9].

Each LPM or compartment can be represented as a combination of resistors, capacitors and inductors which are parameterised by numerical values R, C and L, respectively. For a generic vessel or organ located in a larger

circulation network, R, C and L represent haemodynamic dissipation, vessel distensibility and the inertial effects of the blood flow, respectively [10]. Along with the input parameters of the heart chambers and valves, these parameters form a set of clinical biomarkers, which when personalised to a patient, by integrating patient-specific clinical data, provide the insight that a cardiovascular DT aims to achieve [11].

Useful clinical data are scarce resources, thus the requirement to identify and choose what data are needed to personalise a LPM (in order to create a useful cardiac DT) is a complex one [12]. Within a clinical setting, there are often a range of both continuous and discrete measurement data. But the process of obtaining insightful and diagnostically useful clinical data often requires a series of invasive tests being conducted on the patient. With any data collected (e.g., blood pressure, flow and volume for each compartment), one then generates a series of clinical metrics: ejection fraction [13], to quantify heart failure; pulse pressure [14], to diagnose arterial stiffening; maximum blood velocity [15], to evaluate heart valve stenosis; cardiac output [16], to measure overall heart health and the observation of various clinical time series waveforms [17]. These metrics can then be amalgamated into a DT, enriching the model's predictions with additional detail and validity. However, given the plethora of available clinical tests, each carrying its own risks to patients, determining which metrics are indispensable in creating a faithful virtual representation of a patient becomes a challenging task. Each set of measurements collected and utilised to perform DT related tasks is denoted an experimental design [18].

The integration of clinical data into an LPM to form a DT, is a task denoted 'the personalisation process' (or 'model personalisation' or 'model calibration'). Mathematically, this is also known as the 'inverse problem' [19]. One can think of the solution to the personalisation process as an input parameter set that locates the global minimum of a response surface, spanned by the combination of input parameters of the mechanistic model and the available clinical measurements. Thus, we obtain a set of unique clinical biomarkers [20], i.e we have found a point in the input parameter space such that the outputs of our mechanistic model most closely match the clinical measurements of a patient. It is this point in the input parameter space which describes a patient's patho/physiological state.

Despite progress, there are still many open questions surrounding the personalisation process, which we distil as explicit questions below:

1. What clinical data must be acquired *in-vivo* to obtain insightful, patient-specific biomarkers?
2. Does the set of biomarkers obtained remain consistent in the presence of new and varying experimental designs?
3. What is the computational cost associated with finding the solution of the personalisation process under different experimental designs?
4. Should DTs be built to encapsulate a patient's "physiological envelope" or should DTs be targeted to specific conditions?
5. What are the best practices involved in model personalisation under uncertainty?

This study investigates to what extent the above can be answered. Before proceeding, it is important to note that all investigations in this work are conducted with forward generated model data, in order to understand and extract the clinical biomarkers from the model in an ideal setting, to eliminate any confounding effects of noise in clinical data. The clinical data obtained *in-vivo* influences the in-silico data obtained from the model. Without this critical, off-line step, misleading results may be obtained which could then lead to ill-informed clinical decisions.

The structure of this paper is as follows. In section 2, we: (i) review relevant literature, (ii) introduce concepts germane to the personalisation process in both extraction and optimisation of clinical biomarkers, (iii) detail the position this type of investigation has in the personalisation process and (iv) summarise the principal contributions of this work. In section 3, the mathematical detail is provided for each tool used for model analysis (Sobol indices, identifiability analysis and sloppy analysis). We also present the various experimental designs utilised within this work. Section 4 declares our results from different computational experiments. Discussion of the impact of varying experimental designs on the personalisation process is given in section 5.

2 Foundations & state of the art

Model personalisation is synonymous with the base concepts of input parameter sensitivity, identifiability and sloppiness [21]. From the discussion in section 1, it is prudent to review terminologies, prior art and state how this work will provide a novel insight into the study of model personalisation.

2.1 Terminologies

When attempting to personalise a cardiovascular model, it is important to discuss the prerequisite properties corresponding to input parameter influence (sensitivity), uniqueness (identifiability) and response surface structure (sloppiness).

2.1.1 Sensitivity

An input parameter's effect needs to be influential on the output response surface, if this is the case an input parameter is regarded as **sensitive** [22], i.e., a change in the input parameter space causes a detectable change on the desired output. Thus, the said sensitive input parameter may serve as a clinically insightful biomarker for personalisation (in the creation of a digital twin), due to the ease of capturing the biomarkers' effects in clinical outputs. One can distinguish locally and globally sensitive input parameters, with respect to the measurements. Locally sensitive input parameters are those eliciting the steepest gradient in the output about the model base operating point [23]. Globally sensitive input parameters are potential bio-markers which operate within a physiologically realistic value range. Input parameters are said to be most globally sensitive when they cause the greatest influence on the outputs, for the prescribed parameter ranges [24]. Different methods exist to calculate the sensitivity of input parameters, with the most common being the variance based methods, which we adopt in this work (see section 3.3). The personalisation process and the use of cardiovascular DTs is a global process, because we need a virtual representation of patients in a range of physiological and pathophysiological conditions. Thus, global sensitivity analysis presents itself as an insightful tool in the search for of clinical biomarkers.

2.1.2 Identifiability

Personalisation of models now entails the pursuit of an identifiable model and identifiable input parameters (an optimal subset, denoted as clinical bio-markers). The analysis of identifiability in a cardiovascular system model requires three distinct examinations: structural, sensitivity-based, and practical identifiability. Structural identifiability (theoretical) assumes abundant and noise-free target output data, rendering a model's structural identifiability largely academic in clinical terms. However, this assumption overlooks the possibility that inability to identify input parameters may stem from the model's structure rather than data issues [25]. Naturally, if a model lacks structural identifiability, practical attempts at its utilisation are inherently limited. Sensitivity-based identifiability analysis involves the identification of sensitive and orthogonal input parameters, under synthetic data generated by the model, to ascertain which input parameters are identifiable under ideal circumstances [26]. Practical identifiability analysis takes into account of the quality of patient data, where noise and sampling rates may impact the identification of unique input parameters [27]. For complete personalisation, each stage must be executed sequentially. Within this work, we examine the identifiability of input parameters through their average influence across output space.

2.1.3 System Sloppiness

System sloppiness is a term used to characterise the structure of the input parameter space [28]. As discussed above, the main aim in many areas of systems biology is to optimise a dynamical system's input parameters to available experimental data. This is normally performed by minimising a cost function, to obtain a point in the input parameter space corresponding to a global minimum of the cost function J [29], of the form

$$J(\underline{p}) = \sum_i (y_i(\underline{p}, t) - y_i^e)^2,$$

where $\underline{p}$ is the input parameter set, y_i^e represents the ith experimental measurement available and $y_i(\underline{p}, t)$ represents the ith dynamical system output (obtained from the model), which the experimental data are compared against.

Consider an example dynamical system with two input parameters $p1$ and $p2$. When optimising such a system to experimental data, contour plots displaying the closeness of fit are generated as in figure 1. Here we see that moving up (in the direction of $p2$) and left in the parameter space rapidly changes the value of the cost function, i.e., indicating how good a fit is obtained by a specific value of $p2$. This direction is denoted a stiff direction in the input parameter space. Conversely, if one was to travel up and right (in the direction of $p1$), one could visit a range of $p1$ values without incurring changes of the cost function values. This means the manifold generated by $p1$ is largely linear whereas the one generated by $p2$ has steep gradients leading to a unique global minimum. Thus the sloppy direction controlled by $p1$ would not make for a good biomarker to calibrate a model due to the limited impact of $p1$ to the selection of model outputs. The converse is true for $p2$. However, most models in systems biology and in cardiovascular modelling cannot be visualised through a two dimensional contour map. Mathematical sloppiness analysis of our cardiovascular models can be found in section 3.6.

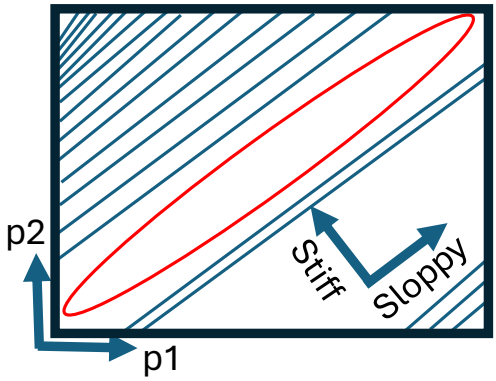

Figure 1: **A two dimensional sloppy model representation:** A two dimensional contour plot displayed as a blue curve, with the minimum contour value displayed in red for input parameters $p1$ and $p2$. Moving up and left would lead to rapid changes in the contour where as moving up and right would lead to slow changes.

The final stage of personalisation is the optimal estimation of selected input parameters, fitted to patient-specific clinical data. Before this optimisation takes place, if we can quantify the stiffness/sloppiness present within the systems input parameter space, it would provide insight into the complexity of the system, and in turn facilitate the choice of optimisation routine (i.e. gradient descent, particle swarm genetic algorithms, unscented Kalman filter) [30, 31].

The related concepts of identifiability and sloppiness provide different but insightful information about the personalisation process [32]. Identifiability is a binary situation, whilst sloppiness quantifies the difficulty associated with obtaining precise identifiable input parameters. The sloppiness analysis of a model can either distinguish stiff and sloppy regions of the input parameter space, or show that the whole system under investigation can be regarded as sloppy. Note, most system biology models belong to the latter category [33, 34]. Within this work, we examine the sloppiness associated with the sensitivity matrices, which are defined by input parameter effects on the chosen outputs. Therefore, we can also establish a secondary aim of investigating the effects of differing experimental design on a cardiovascular system sloppiness.

2.2 Relevant Literature

Cardiovascular model personalisation has been attempted in many clinically important areas such as, congenital heart disease, fetal circulation or whole heart multi-scale modelling [35, 36, 37]. In the majority of works, standard optimisation routines are used to obtain a set of input parameters which are representative of the experimental data [38, 39, 40]. Outside of the standard optimisation routines, data assimilation methods, namely ensemble and unscented Kalman filters, have developed traction as an efficient way to estimate patient specific input parameters, at a reduced cost, compared to the optimisation methods [41, 42, 31]. Another area which attracted research community's attention recently is the utilisation of sensitivity analysis to guide the search and selection of an optimal input parameter subset for simpler and more efficient parameter estimations. Colunga et al. [43] applied this technique to incorporate invasive right heart data to obtain the personalisation of a model of pulmonary hypertension with 25 parameters. Where as Strocchi et al. [44] applied global sensitivity analysis to a 117-parameter cell-to-organ 4-chamber heart representation, reducing the model down to 45 personalisable parameters. Schafer et al. [45] examined how the sensitivities in a 1D model of the carotid artery change with respect to age and sex, highlighting how the input parameters for personalisation do not remain constant.

As discussed above, it is also important to understand the identifiability of input parameters, because this provides reassurance that any optimised input parameters are unique to a patient. Casas et al. [46] performed a profile likelihood analysis of a LPM to personalise flow in the systemic circulation. In comparison, other researchers such as Pironet et al., [47, 48] performed a structural and sensitivity identifiability analysis on a LPM to highlight what outputs would be required to obtain unique input parameters. In addition, there have been developments of experimental approaches from Marquis et al., de Bournonville et al. and Sala et al., who used invasive patient data to make good first estimates of model input parameters before optimisation which ensured more input parameters within the model are identifiable [49, 50, 51].

Another popular approach was to optimise input parameters in an iterative manner [52]. Bjordalsbakke et al.

[53] applied an iterative step-wise reduction scheme in which, guided by sensitivity analysis, they began to optimise a group of parameters with increased number, each time with different cost functions to examine the closeness of fit. Bjordalsbakke [53] found that cost functions constructed from waveform data, as opposed to common clinical metrics, produced the smallest errors. Hann et al. [54], took a similarly structured approach in reducing the number of available outputs to reduce the complexity associated with the model. They demonstrated that differing measurement sets consisting of continuous and discrete measurements allowed for each subsection of the model to be optimised with minimal error. The impact of varying outputs have also been examined by Eck et al. [55] through uncertainty quantification in the arterial wall models and concluded that continuous time series Sobol indices gave a more insightful look into the process.

All studies above indirectly examined the impact of changing outputs on obtaining personalisable input parameter sets. However this was not the primary objective of their investigations. The most notable publication to date which investigated the impact of experimental design on a cardiovascular model was that of Colebank et al. [56]. They studied the impact of 4 different experimental designs on the ventricular function and found easily identifying biomarkers of the ventricular function, when a practical identifiability analysis is performed (including continuous data from both the left and right side of the heart).

Another aim of our study is to reveal and analyse the impact of experimental designs on system sloppiness. Sloppiness is a property which has been known in system biology models for over a decade [33]. Most studies have been focused on pharmacokinetic models [57] and examinations of the route cause of sloppiness. More recently, a formal definition of sloppiness was given and the concept was used to obtain a minimum set of outputs to ensure identifiability [58, 59]. The impact of experimental designs on system sloppiness has been understood through the lens of model identifiability (i.e., varying the model and the data shown to the model can induce different intensity of model sloppiness which in turn impacts the overall identifiability of the model parameters) [60, 61, 62]. In terms of cardiovascular modelling, sloppy analysis has been applied to electrophysiology modelling with the focus on calcium and potassium channel modelling. Whitterker et al. [63], utilised sloppy analysis to provide a method to simplify complex models of ion channels that improves parameter identifiability which will aid in future development in voltage-gated ion channels. Sloppy analysis has been applied to other classes of biochemical models [64, 65]. For example, Bravo et al. [34] applied sloppy analysis to a Bayesian model of an electrophysiological process to highlight how the identification of stiff parameter combinations made the model personalisation much simpler. As far as we are aware, sloppy analysis of a mechanical LPM of the cardiovascular system has not been performed, nor has the impact of varying experimental designs on sloppiness been studied.

2.3 Rationale and Contributions

DTs in cardiovascular medicine offer profound promise in improving patient care. In order to advance the application of DTs in clinic, further study into the impact of experimental designs on the personalisation process must be understood. We investigate the impact of varying clinical metrics, both continuous and discrete, in an ideal scenario (without the bias of measurement noise). The main contributions of the work are:

1. **Stability of identifiable parameters:** Through varying experimental designs, we investigate changes in the identifiability ranking of input parameters.
2. **Sloppy analysis of an LPM:** We perform and report the first global sloppy analysis of a cardiovascular LPM to aid our understanding of the personalisation process.
3. **Clinical metric guidelines:** By evaluating different clinical metrics, we provide insight into the set of clinical data (and therefore measurements) needed for the effective personalisation of cardiovascular models.

By rigorously assessing the impact of varying clinical metrics and performing the first insightful sloppy analysis of a cardiovascular model, revealing the structure of the input parameter space, our work furthers the investigation and understanding needed in the personalisation of cardiovascular DTs.

3 Methods

Here, we examine the methods used for analysing a 4-chamber cardiovascular circulation model. In section 3.1, we present the 4-chamber model, explain the computational framework and provide a full parameterisation with their initial conditions. We then detail the clinical measures utilised in this work, which map to the different measurement sets in section 3.2. The global sensitivity method of Sobol indices and the related Fisher information matrix are given in section 3.3 and section 3.4 respectively. In section 3.5, we then examine an average metric for input parameter influence. We detail how to examine system sloppiness in an $n-$dimensional space in section 3.6. Finally, section 3.7 is devoted

to highlight the iterative workflow we devised to examine the effects of varying experimental design on input parameter influence and sloppiness.

3.1 Cardiovascular Model

Our LPM can be expressed in a standard state space formulation:

$$\frac{d}{dt}\underline{X}(t) = \underline{f}\left(\underline{X}(t); \underline{p}\right), \quad \underline{Y}(t) = \underline{h}(\underline{X}(t)), \tag{1}$$

in which $\underline{p}$ denotes an input parameter vector, $\underline{X}$ represents the set of state variables of the system, $\underline{f}$ is a function describing the system (usually this is an collection of differential algebraic equations), $\underline{h}$ is the measurement function where the forward model synthetic measurements are generated, using the computed state variables $\underline{X}$, and $\underline{Y}$ represents the measurements of interest.

The model declared in its electrical analogue form in figure 2 is a system-set, differential algebraic equation based, electrical analogue cardiovascular model, after Comunale et al., [66], with 4 heart chambers and a representation of both the systemic and pulmonary circulations. The model was first developed to model both physiological and pathophysiological states. The state variables of each compartment are specified by its time-dependant dynamic pressure P (mmHg), inlet flow Q (mL/s) and volume V (mL):

$$X_k(t) = (V_k(t), P_k(t), Q_k(t)), \quad k \in \{la, lv, sa, svb, sv, ra, rv, pa, pvb, pv\}, \tag{2}$$

where la denotes the left atrium, lv denotes the left ventricle, sa the systemic arteries, svb the systemic vascular bed, sv the systemic venous system, ra the right atrium, rv the right ventricle, pa the pulmonary arteries, pvb the pulmonary vascular bed and pv the pulmonary venous system, Formally, t is a continuous time variable.

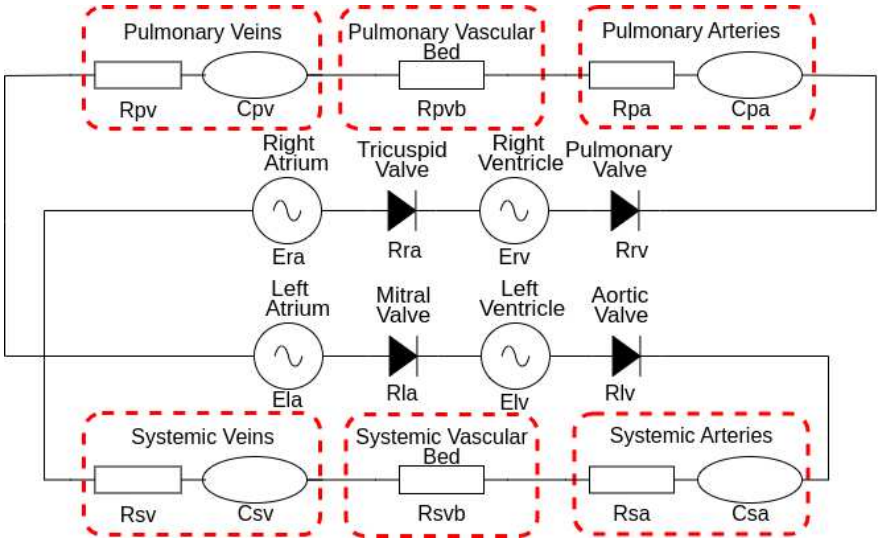

Figure 2: **4-Chamber cardiovascular model**: Our state-space cardiovascular model, first introduced by Comunale et al. [66]. Both left and right atria and ventricles are represented by the Shi double cosine model [67]. Heart valves are assumed to have Ohmic behaviour allowing no back flow. The systemic and pulmonary circulations are represented by a CRRCR combination with all parameters are given in table 1.

In generic form, the equations relating to the passive compartmental state variables all take the form:

$$\frac{dV_{s,k}}{dt} = Q_k - Q_{k+1}, \quad \frac{dP_k}{dt} = \frac{1}{C_k}(Q_k - Q_{k+1}), \quad Q_k = \frac{P_{k-1} - P_k}{R_k}. \tag{3}$$

Above, the subscripts $(k-1), k, (k+1)$ respectively represent the proximal, present and distal system compartments; $V_{s,k}$(mL) denotes the circulating (stressed) volume [68] and C_k (ml/mmHg) and R_k (mmHgs/mL) denote compartmental compliance and the Ohmic resistance between compartments k, $(k+1)$. Flow in and out of the active heart chambers are controlled by Ohmic diode valves:

$$Q_k = \begin{cases} \frac{P_{k-1} - P_k}{R_{val}}, & P_{k-1} > P_k, \\ 0 & P_{k-1} \leq P_k, \end{cases} \tag{4}$$

where $R_{val} = (R_{lv}, R_{la}, R_{rv}, R_{ra})$ representing the resistances across aortic, mitral, pulmonary and tricuspid valves. The active heart chambers can be represented by time varying elastances $E_k(t)$ (mmHg/ml), which determines the change in pressure for a given change in the volume [68]:

$$E_k(t) = \frac{P_k(t)}{V_k(t) - V_{k,0}} = \frac{P_k(t)}{V_{k,s}(t)}, \quad k \in \{lv, rv, la, ra\} \tag{5}$$

where $V_{k,0}$ & $V_{k,s}(t)$ represent the chamber unstressed and stressed volumes for the two ventricles and atria. $E_k(t)$ is written following [67]:

$$\begin{aligned} \tilde{t} &= \text{Mod}(t + (1 - E_{k,shift})\tau, \tau) \\ E_k(\tilde{t}) &= (E_{k,max} - E_{k,min}) \cdot e(\tilde{t}) + E_{k,min}, \\ e(\tilde{t}) &= \begin{cases} \frac{1}{2}\left[1 - \cos(\frac{\pi \tilde{t}}{\tau_{k,es}})\right], & 0 \leq \tilde{t} < \tau_{k,es}, \\ \frac{1}{2}\left[1 + \cos(\frac{\pi(\tilde{t} - \tau_{k,es})}{\tau_{k,ep} - \tau_{k,es}})\right], & \tau_{k,es} \leq \tilde{t} < \tau_{k,ep}, \\ 0, & \tau_{k,ep} \leq \tilde{t} < \tau, \end{cases} \end{aligned} \tag{6}$$

where $e(t; \tau_{k,es}, \tau_{k,ep}, E_{k,shift})$ is the activation function for the heart chamber and is parameterised by the end systolic and end pulse timing parameters $\tau_{k,es}$ and $\tau_{k,ep}$ respectively.

Table 1 provides the parameterisation for the model to produce physiological results for the 4-chamber model in which the input parameter space has a dimensionality of 36. To construct the model, the cardiovascular LPM Julia package CirculatorySystemModels.jl [69] is utilised which reduces the system to 8 ordinary differential equations in volume with the initial volumes also given in table 1. The model is solved utilising the Vern7 [70] algorithm with tolerances of $1e^{-6}$. For 30 cardiac cycles the model computes in 0.064s.

3.2 Clinical Measures

When varying the experimental design, we adopt medically accurate measures which are utilised in diagnosing cardiovascular issues. To investigate the effect of experimental design, we devise an additive algorithm: each time we move to a new measurement set, we add the new measurement to the previous output set and therefore defining a new output space of increased dimension, for the analysis of input parameter effects. Practically, the below outputs represent the conventional tests which a patient may be subjected to, with increasing invasiveness to assess their cardiovascular health. While we do not target a specific condition in this work the increasing output sets represent further and deepening knowledge about a patients physiological envelope.

In tables 2, 3 and 4, we display the various measurement sets for the cases of discrete, continuous and mixed measurement sets.

3.2.1 Discrete Measurements

In the discrete case in table 2, we utilise only single point metrics. These metrics can be obtained through just 3 clinical tests:

1. Blood Pressure (BP): This can be readily obtained through a sphygmomanometer reading while a patient is in hospital. In our chosen model, this measurement is obtained by calculating $\frac{\text{Max}(P_{sa})}{\text{Min}(P_{sa})}$ and corresponds to set 1.
2. Ejection Fraction (EF): This can be obtained through an echocardiogram. In our model, we calculate EF for the left and right ventricle then the left and right atria as $\frac{\text{Max}(V_i) - \text{Min}(V_i)}{\text{Min}(V_i)}$. For $i = lv, rv, la, ra$ this corresponds to sets 2A, 2B, 2C and 2D.
3. Max(Q_i) - Maximum flow: This could be obtained from either an echocardiogram or a cardiac MRI. This is calculated for the systemic arteries, pulmonary arteries, aortic valve, mitral valve, pulmonary valve and tricuspid valve.

To highlight the additive process of the experiment in the discrete setting, for example, the full output set for 3A is defined as follows:

$$\text{Set 3A} = (BP, EF_{lv}, EF_{rv}, EF_{la}, EF_{ra}, \text{Max}(Q_s)).$$

Table 1: **Input parameters for the 4 chamber model:** Each input parameter is displayed along with the respective units and valves. Here we fix the heart period cycle to $\tau = 0.81(\text{s})$.

Heart Parameters					
Parameter Name	Symbol	LV	RV	LA	RA
Maximal Elastance $[mmHg/ml]$	E_{max}	2.8	0.45	0.13	0.09
Minimal Elastance $[mmHg/ml]$	E_{min}	0.07	0.035	0.09	0.045
Unstressed Volume $[ml]$	V_0	20	30	3	7
End Systolic Time $[s]$	τ_{es}	0.269τ	0.269τ	0.11τ	0.11τ
End Diastolic Time $[s]$	τ_{ep}	0.452τ	0.452τ	0.18τ	0.18τ
Atrial Activation Time $[s]$	E_{shift}	0	0	0.85τ	0.85τ
Valve Resistance $[mmHg \cdot s/ml]$	R_{val}	0.01	0.01	0.005	0.005

Circulation Parameters			Initial Volume Values		
Resistance Systemic Arteries $[mmHg \cdot s/ml]$	R_{sa}	0.0448	Initial Volume Systemic Arteries $[ml]$	$V_{sa,0}$	98.3
Resistance Systemic Vascular Bed $[mmHg \cdot s/ml]$	R_{svb}	0.824	Initial Volume Systemic Veins $[ml]$	$V_{sv,0}$	117.996
Resistance Systemic Veins $[mmHg \cdot s/ml]$	R_{sv}	0.0269	Initial Volume Pulmonary Arteries $[ml]$	$V_{pa,0}$	100.5
Resistance Pulmonary Arteries $[mmHg \cdot s/ml]$	R_{pa}	0.003	Initial Volume Pulmonary Veins $[ml]$	$V_{pv,0}$	126.4
Resistance Pulmonary Vascular Bed $[mmHg \cdot s/ml]$	R_{pvb}	0.0552	Initial Volume Left Ventricle $[ml]$	$V_{lv,0}$	149.6
Resistance Pulmonary Veins $[mmHg \cdot s/ml]$	R_{pv}	0.0018	Initial Volume Right Ventricle $[ml]$	$V_{rv,0}$	189.2
Compliance Systemic Arteries $[ml/mmHg]$	C_{sa}	0.983	Initial Volume Left Atrium $[ml]$	$V_{la,0}$	71
Compliance Systemic Veins $[ml/mmHg]$	C_{sv}	29.499	Initial Volume Right Atrium $[ml]$	$V_{ra,0}$	67
Compliance Pulmonary Arteries $[ml/mmHg]$	C_{pa}	6.7			
Compliance Pulmonary Veins $[ml/mmHg]$	C_{pv}	15.8			

Discrete Measurement Sets						
Set	1	2A	2B	2C	2D	
Measurement Added	BP	EF_{lv}	EF_{rv}	EF_{la}	EF_{ra}	
Set	3A	3B	3C	3D	3E	3F
Measurement Added	Max(Q_s)	Max(Q_p)	Max(Q_{lv})	Max(Q_{la})	Max(Q_{rv})	Max(Q_{ra})

Table 2: **Table of Discrete Measurements:** Each discrete measurement set shows which new measurement is added to the increasing output set, along with all existing measurements. Each discrete measurement equates to a single point extracted from the cardiac cycle.

3.2.2 Continuous Measurements

For the continuous measurements displayed in table 3, each continuous waveform obtained is made up of 150 time points. This metrics can be obtained though 4 clinical metrics below.

1. Q_i - Flow rate: This can be obtained through a Doppler ultrasound, for the systemic, pulmonary, aortic valve, mitral valve, pulmonary valve and tricuspid valve.
2. V_i - Chamber volume: can be obtained through a cardiac MRI, for the two ventricles and two atria.
3. P_{lv}, P_{sa} - Left heart pressures: These invasive diagnostic measurements can be obtained through catherterisation for the left ventricle and systemic artery.
4. $P_{rv}, P_{pa}, P_{ra}, P_{pv}$ - Right heart and circulation pressures: These invasive measurements can be obtained by performing Swan-Ganz catherterisation and wave form pressures are collected in the right heart for the right ventricle, pulmonary artery, right atrium and pulmonary vein (which can also be seen as a surrogate for left atrial pressure).

Continuous Measurement Sets						
Set	1A	1B	1C	1D	1E	1F
Measurement Added	Q_s	Q_p	Q_{lv}	Q_{la}	Q_{rv}	Q_{ra}
Set	2A	2B	2C	2D	3A	3B
Measurement Added	V_{lv}	V_{rv}	V_{la}	V_{ra}	P_{lv}	P_{sa}
Set	4A	4B	4C	4D		
Measurement Added	P_{rv}	P_{pa}	P_{ra}	P_{pv}		

Table 3: **Continuous Measurement Table:** Each continuous set shows which new measurement is added to the increasing output set, along with all measurements that have appeared before. Each continuous measurement equates to a single converged cardiac cycle, consisting of 150 time points.

3.2.3 Mixed Measurement Sets

The previous two measurement settings will reveal the difference between continuous and discrete metrics. The mixed measurement set combines both the discrete and continuous measurements but represents a standard diagnosis procedure with increasing invasiveness, i.e., in clinic, a patient would not be subject to invasive chamber pressure measurements unless deemed necessary. Apart from one additional measurement (noisy blood pressure) which will be introduced bellow, all other metrics and corresponding measurement sets are the same as the ones defined in sections 5 and 6.

- BPN - noisy blood pressure: This set is added to represent the situation of a patient taking their own arterial blood pressure measurement at home, with noisy reading due to potential human error and lower device accuracy. The analysis of noisy output data will provide insight into how global sensitivity indices alter in the presence of noise.

BPN is calculated as

$$\text{BPN} = \frac{\text{Max}(P_{sa})}{\text{Min}(P_{sa})} \times (1+\epsilon), \quad \epsilon \sim N(0, 0.1).$$

In this setting, set 2 represents an arterial blood pressure measurement obtained in hospital and is assumed to not be subject to noise. Slightly different to the measurement sets introduced in sections 5 and 6, here set 2 will replace set 1 instead of adding to it and set 2 will be used in all increasing measurement sets for the later sets.

3.3 Sobol indices

Given a model of the form in equation 1 with Y (a continuous or discrete output), a variance based first order or total order effect can be calculated for a generic input factor p_i. p_i^c denotes the complementary set, i.e., all other model inputs excluding p_i. Performing a Sobol analysis provides the quantification of the input parameter effect against a specific output [71]. Both the first and total order sensitivity indices return a matrix of the form:

$$\boldsymbol{S} = S_{j,i}, \ j = 1, ..., m; \ i = 1, ..., n, \tag{7}$$

Mixed Measurement Sets						
Set	1	2	3A	3B	3C	3D
Measurement Added	BPN	BP	EF_{lv}	EF_{rv}	EF_{la}	EF_{ra}
Set	4A	4B	4C	4D	4E	4F
Measurement Added	Q_s	Q_p	Q_{lv}	Q_{la}	Q_{rv}	Q_{ra}
Set	5A	5B	5C	5D	5E	
Measurement Added	Max(Q_{lv})	Max(Q_{la})	Max(Q_{rv})	Max(Q_{ra})	V_{lv}	
Set	5F	5G	5H	6A	6B	
Measurement Added	V_{rv}	V_{ra}	V_{ra}	P_{sv}	P_{sa}	
Set	7A	7B	7C	7D		
Measurement Added	P_{rv}	P_{pa}	P_{ra}	P_{pv}		

Table 4: **Table of Mixed Measurement:** Each set shows which new measurement is added to the increasing output set (apart from set 2 which replaces set 1) along with all measurements that have appeared before. Each discrete measurement added constitutes to a single point extracted from the cardiac cycle. For each continuous measurement added, this constitutes to a converged cardiac cycle made up 150 time points.

where n and m represent the number of input parameters and output measurements, respectively. In this work, we handle a fixed high-dimensional input parameter space ($n = 36$). However, when the experimental design changes, m varies and also the output measurement space. For example, in the discrete measurement setting, the largest value of m is 11. In comparison, in the mixed measurement setting, the largest output set (set 7D) results in $m = 1609$, so the resulting sensitivity matrix is of size $\boldsymbol{S} = (1609 \times 36)$.

The first and total order sensitivity indices can be written as:

$$S_{1,i}(Y) = \frac{\text{Var}(\text{E}(Y|p_i))}{\text{Var}(Y)}, \quad S_{T,i}(Y) = \frac{\text{E}(\text{Var}(Y|p_i^c))}{\text{Var}(Y)}, \tag{8}$$

where $S_{1,i}$, $S_{T,i}$ denote the first and total order indices' vectors for an input parameter p_i against the specific output Y. In order to quantify the effects continuous measurements have on the calculation of sensitivity indices, we typically average this sensitivity waveform. Rather than averaging across a time range (which process regions of low variance equally to those of high variance), one seeks to expose differential sensitivities by examining variance-weighted averages:

$$TAS_i = \frac{\sum_k S_i(\underline{Y}^c(t_k))\text{Var}(\underline{Y}^c(t_k))}{\sum_k \text{Var}(\underline{Y}^c(t_k))}, \tag{9}$$

where TAS_i is the time averaged first/total order effect of an input parameter i and $\underline{Y}^c(t_k)$ represents the approximated continuous measurement at time step k [55].

The sensitivity indices can be interpreted as:

$$S_{T,i} = S_i + \sum_{i \neq j} S_{ij} + \sum_{i \neq j \neq k} S_{ijk} + ...,$$

i.e., for a given input parameter p_i, the total order indices are the first order indices (p_i's independent effects) *plus* all higher order interactions. This study utilises the total order sensitivity matrix to quantify an input parameter's full impact on the outputs. To ensure convergence, we used $75,000$ samples with the Jansen estimator [72, 73] with a bootstrapping sample of 1000 [74].

3.4 Fisher Information

Another important matrix derived from the $(m \times n)$ sensitivity matrices is the square $(n \times n)$ Fisher information matrix (FIM) [75]:

$$\boldsymbol{F} = \mathbf{S}^T\mathbf{S}. \tag{10}$$

The FIM is a symmetric matrix representing the information one can extract on parameters from the model outputs (i.e., the available measurements [76]). We choose to construct the FIM from the total order Sobol indices (equation 8) to

account for the full non-linear effects which are present within the system and the impacts of the varying experimental designs as done in poreviosu work [77, 23, 78].

3.5 Average Parameter Influence

The sensitivity vectors derived in section 3.3 only display the effects of an input parameter against a specific measurement. In order to obtain an input parameter's identifiability, we must assess an input parameter's influence across our chosen set of outputs. Li et al., [79], derived such a metric based upon the FIM $\boldsymbol{F}$ defined in equation (10). To examine the global effect of input parameters through the FIM, we use principal component analysis (PCA) [80] where the principal components (PC) are the eigenvectors of the FIM.

Let $\boldsymbol{Q}$ be the matrix of the ordered PC (eigenvectors of $\boldsymbol{F}$), in which the absolute value of each element Q_{ij} reflects the contribution of the i^{th} parameter to the variance of the jth output. We follow Li et al. [79], who measure an overall effect for the i^{th} parameter as:

$$E_i = \frac{\sum_{j=1}^{m} |\mu_j Q_{ij}|}{\sum_{j=1}^{m} |\mu_j|}, \tag{11}$$

where $0 \leq E_i \leq 1$ and μ_j represents the non-zero eigenvalues of $\boldsymbol{F}$. This measure reflects the difficulty in determining the i^{th} parameter when only a single factor is estimated. Parameter identifiability is associated with E_i - the larger the value of E_i, the more identifiable the i^{th} parameter is. We record the rank and the overall effect of every input parameter greater than 0.01, a number which has been discussed as the lowest possible value that may have the possibility of being identifiable in [23].

3.6 Sloppiness Analysis

In section 2.1.3, we explored the concept of sloppiness by examining the contour lines of the cost function. In order to examine sloppiness in an n-dimensional input parameter space, we examine the eigenvalues of FIM (equation 10). The eigenvalues of the FIM provide insight into the variation of parameters constrained by the available data. A model can be regarded as sloppy if the eigenvalues of the FIM have a uniform spacing on a log scale spread over many orders of magnitude [28, 61, 81, 82]. On the other hand, if the FIM eigenvalues have a non-uniform distribution, the model is regarded as stiff. We can then identify stiff directions in the input parameter space which corresponds to a set of input parameters where personalisation should take place.

One can interpret this analysis as follows, the eigenvalues of the FIM represents the variation that a model parameter contributes the model outputs. In the case where a model is stiff we have a select subset of model parameters with large eigenvalues compared to their complementary set. Thus when looking to calibrate model parameters this stiff subset of input parameters denote rapidly varying directions on the response surface, thus one can more easily obtain a personalised operating point of input parameters, due to the impact of varying input parameter sets been clear. Conversely in the case of sloppy models these properties are not clear in the response surface thus choosing the correct direction for personalisation more difficult.

3.7 Workflow

All the above sections define an iterative investigation in which we examine the effects of varying experimental designs on input parameter's influence and sloppiness. This can be encapsulated in the following steps and in figure 3.

1. Define an output set: As shown in section 3.2, we define the various sets of discrete, continuous and mixed measurements, starting from the first and simplest output set.
2. Calculate S_T: Form the total order sensitivity matrix for the input parameters and chosen output set.
3. Form the FIM: Utilising equation 10, the FIM represents all the information about the parameters constrained by the specific measurement set.
4. Analyse parameter's influence and sloppiness: Using methods in section 3.5 and 3.6, we record each input parameter's rank and influence value being greater than 0.01 and the distribution of eigenvalues.
5. Add a new measurement: Move to the next measurement set and repeat stages 2-4.

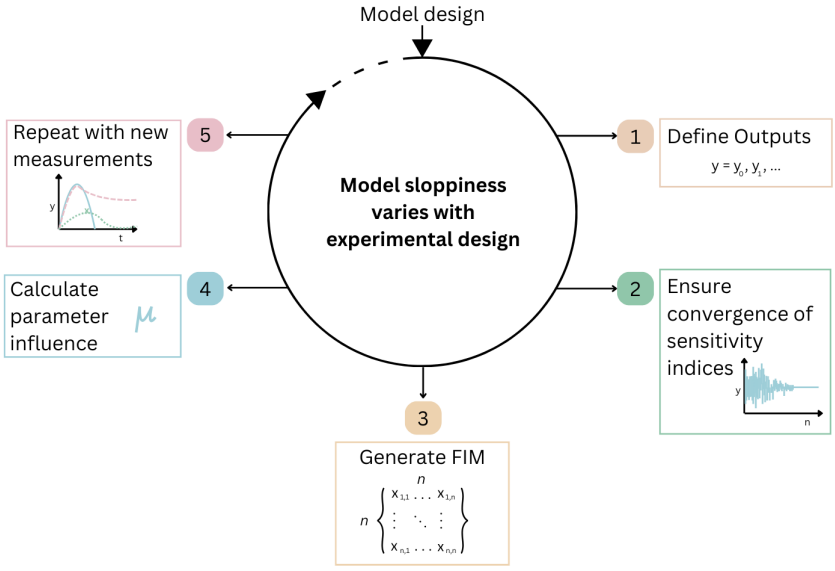

Figure 3: **Experimental Design Workflow**: The process for how to analyse the input parameter influence and sloppiness in the presence of changing experimental designs.

4 Results

Sections 4.1, 4.2 and 4.3 detail the average input parameter influence across all outputs for varying experimental design, using the method presented in section 3.5. The average input parameter rank and values are displayed as tables. The corresponding figure in each section displays the eigenvalues of the Fisher information matrix on a $\log_{10}$ scale, for varying measurement sets (see sections 3.4 and 3.6). The sections below presents results for the varying discrete, continuous and mixed measurement sets, respectively, as described in section 3.2.

4.1 Discrete Measures

Table 5 displays the rank of each input parameter and their corresponding influence value calculated using equation 11, using discrete measurements. We note, from set 1 to set 3F, the resistance of the systemic vascular bed R_{svb} and the systemic arterial compliance C_{sa} rank the highest, with the largest influence values, with the exception from set 2D in which $E_{shift,ra}$ ranks the most influential. This can be explained by the experimental design. The newest measurement added for set 2D was the ejection fraction of the right atrium. Although in all the other cases, it appears R_{svb} and C_{sa} still dominate. As more measurements are added to the experimental design, we observe more input parameters record an influence score greater than 0.01. For case 3F where there are 11 outputs, 17 input parameters are recorded with an influence score larger than 0.01. As the measurement set increases, the largest influential value decreases. In addition, as more measurements are added, although more “influential" parameters are obtained, the majority have an influence score in the range of hundredths.

The sloppy analysis result in figure 4 shows that the model cannot be regarded as sloppy, with a discrete output set. With an increasing output set, we observe more input parameters are regarded as stiff. Even with the largest output set, set 3F, the model still exhibits an eigenvalue spectrum of over 15 orders of magnitude.

4.2 Continuous Measures

With an increasing continuous measurement set, in figure 6, a much higher number of influential input parameters are present, compared to the discrete case (figure 5). Even with just a single continuous measurement of the systemic flow (Column 1A), 17 input parameters are regarded as influential. In set 4D, where there are 16 continuous output measurements, 20 input parameters are recorded as influential. Here, the ranking of influential input parameters shows much less consistency, compared to table 5. The most influential parameters appear to loosely correlate with the latest

Measurement Sets									
1		2A		2B		2C		2D	
P	E	P	E	P	E	P	E	P	E
C_{sa}	0.80	R_{svb}	0.44	R_{svb}	0.34	R_{svb}	0.26	$E_{shift,ra}$	0.24
R_{svb}	0.60	C_{sa}	0.43	C_{sa}	0.33	C_{sa}	0.26	R_{svb}	0.10
$\tau_{es,lv}$	0.04	$E_{max,lv}$	0.24	$E_{max,lv}$	0.18	$E_{max,lv}$	0.14	C_{sa}	0.10
		$V_{0,lv}$	0.04	$V_{0,lv}$	0.03	$V_{0,lv}$	0.03	$E_{max,lv}$	0.06
		$\tau_{es,lv}$	0.02	$E_{max,rv}$	0.02	$E_{max,rv}$	0.02	$E_{max,ra}$	0.04
				$\tau_{es,lv}$	0.02	$\tau_{es,lv}$	0.01	$\tau_{ep,rv}$	0.02
								$E_{min,rv}$	0.01
								$E_{max,rv}$	0.01
								$V_{0,lv}$	0.01

Measurement Sets											
3A		3B		3C		3D		3E		3F	
P	E	P	E	P	E	P	E	P	E	P	E
R_{svb}	0.22	R_{svb}	0.20	R_{svb}	0.19	R_{svb}	0.17	R_{svb}	0.15	R_{svb}	0.13
C_{sa}	0.20	C_{sa}	0.18	C_{sa}	0.17	C_{sa}	0.15	C_{sa}	0.13	C_{sa}	0.11
$E_{max,lv}$	0.10	$E_{max,lv}$	0.09	$E_{max,lv}$	0.09	$E_{max,lv}$	0.09	$E_{max,lv}$	0.08	$E_{shift,ra}$	0.10
$E_{shift,ra}$	0.05	$E_{shift,ra}$	0.06	$E_{shift,ra}$	0.06	$\tau_{es,lv}$	0.05	$E_{shift,ra}$	0.05	$E_{max,lv}$	0.07
$E_{min,lv}$	0.03	$E_{min,lv}$	0.03	$E_{min,lv}$	0.03	$E_{shift,ra}$	0.05	$\tau_{es,lv}$	0.05	$\tau_{es,lv}$	0.04
$E_{max,rv}$	0.02	$E_{max,rv}$	0.02	C_{pa}	0.03	$E_{min,lv}$	0.03	$E_{min,lv}$	0.05	$E_{min,lv}$	0.03
$V_{0,lv}$	0.02	$V_{0,lv}$	0.01	R_{pvb}	0.03	$E_{max,rv}$	0.02	$E_{max,rv}$	0.03	$E_{max,ra}$	0.03
C_{sv}	0.01	C_{sv}	0.01	$E_{max,rv}$	0.02	$E_{max,la}$	0.02	$\tau_{es,rv}$	0.02	$E_{max,rv}$	0.03
$E_{max,la}$	0.01	$E_{max,la}$	0.01	$E_{shift,la}$	0.02	$E_{shift,la}$	0.02	$E_{max,la}$	0.02	$\tau_{es,rv}$	0.03
$E_{shift,la}$	0.01	$E_{shift,la}$	0.01	$E_{max,la}$	0.02	C_{sv}	0.01	$E_{shift,la}$	0.02	$E_{min,ra}$	0.02
$\tau_{es,lv}$	0.01	C_{pa}	0.01	C_{sv}	0.02	$V_{0,lv}$	0.01	C_{sv}	0.02	C_{sv}	0.02
R_{pvb}	0.01	R_{pvb}	0.01	$V_{0,lv}$	0.01	C_{pa}	0.01	$E_{min,rv}$	0.01	$E_{shift,la}$	0.02
$E_{min,rv}$	0.01	$E_{min,rv}$	0.01	$E_{min,rv}$	0.01	$E_{min,rv}$	0.01	$V_{0,lv}$	0.01	$E_{max,la}$	0.02
$\tau_{es,lv}$	0.01	$\tau_{es,lv}$	0.01	$E_{max,ra}$	0.01	R_{pvb}	0.01	C_{pa}	0.01	$E_{min,rv}$	0.01
						R_{pvb}	0.01	R_{pvb}	0.01	R_{ra}	0.01
										C_{pa}	0.01
										R_{pvb}	0.01

Table 5: **Input parameter ranking for discrete measurements:** Averaging across all output space, the input parameter rank and its respective influence value are displayed, for increasing discrete measurements. Here P represents the parameter and E is the respective average influence value as defined in equation 11.

output added to the measurement list. For example, in set 3B, the left ventricular pressure and systemic arterial pressure are new additions to the output set, and then the top ranking parameters are the minimal ventricular elastance $E_{min,lv}$ and the end pulse time for the left ventricle $\tau_{ep,lv}$. Where as in set 4C, pressures associated with the pulmonary system have just been added, then the top ranking parameters are the right atrial activation time $E_{shift,ra}$ and the minimal elastance for the right ventricle $E_{min,rv}$. Despite the change in rankings, we note that a similar set of input parameters are recorded as influential input parameters, with just minor changes when new output measurements are added. As observed in the discrete measurement set, when more input parameters are regarded as influential, the concentration of influence decreases and is more evenly spread between the input parameters with an influence value greater than 0.01.

Figure 5 shows that for any continuous measurement set, the system can be regarded as sloppy. When increasing the output measurements, the set of sloppiness decreases, with the eigenvalue spectra decreasing from a range of 10^{-16} to 10^{-6}. Compared to the discrete sloppy analysis (figure 4), input parameters in the stiff direction exhibit larger values than observed previously.

4.3 Mixed Measures

When combing both discrete and continuous measurements, the results in table 7 show a similar structure to that observed when only continuous measurements are utilised. When only BPN is the only output, all input parameters record an influence greater than 0.01, despite the noise, there are still clear influence parameters (C_{sa}, R_{svb} and $\tau_{es,lv}$) which could be regarded as biomarkers. However, when we introduce the noise free BP, the influence values associated with the biomarkers increase largely. At set 4A, the first continuous measurement is introduced alongside the previous discrete ones, as a consequence we observe the number of input parameters with influence greater than 0.01 grows from

Measurement Sets											
1A		1B		1C		1D		1E		1F	
P	E	P	E	P	E	P	E	P	E	P	E
$E_{min,lv}$	0.57	$E_{min,lv}$	0.32	$\tau_{es,lv}$	0.38	$E_{shift,la}$	0.21	$E_{shift,la}$	0.19	$E_{shift,la}$	0.11
R_{svb}	0.26	$E_{shift,la}$	0.16	$E_{min,lv}$	0.14	$\tau_{ep,lv}$	0.18	$\tau_{ep,lv}$	0.15	$E_{shift,ra}$	0.1
C_{sa}	0.23	R_{svb}	0.16	R_{svb}	0.1	$E_{min,lv}$	0.07	$E_{min,lv}$	0.06	$\tau_{ep,lv}$	0.08
$\tau_{es,lv}$	0.16	C_{pa}	0.14	C_{sa}	0.06	$\tau_{es,lv}$	0.06	$\tau_{es,lv}$	0.05	$E_{min,lv}$	0.04
C_{pv}	0.15	C_{sv}	0.12	$E_{max,lv}$	0.06	R_{svb}	0.03	$\tau_{es,rv}$	0.05	$\tau_{es,rv}$	0.04
$E_{shift,la}$	0.13	C_{sa}	0.11	$E_{shift,la}$	0.05	C_{pa}	0.03	R_{svb}	0.03	$\tau_{es,lv}$	0.03
$E_{max,lv}$	0.13	R_{pvb}	0.11	C_{sv}	0.04	$E_{min,la}$	0.03	C_{pa}	0.03	$\tau_{ep,rv}$	0.03
C_{sv}	0.12	$\tau_{es,rv}$	0.1	C_{pa}	0.04	C_{sv}	0.02	$E_{min,la}$	0.02	R_{svb}	0.02
$E_{shift,ra}$	0.08	C_{pv}	0.1	C_{pv}	0.04	$E_{max,la}$	0.02	C_{sv}	0.02	C_{pa}	0.02
$E_{max,la}$	0.08	$E_{max,lv}$	0.09	R_{pvb}	0.03	R_{pvb}	0.02	$E_{max,la}$	0.02	C_{sv}	0.02
$E_{min,rv}$	0.08	$\tau_{es,lv}$	0.09	$E_{shift,ra}$	0.03	$\tau_{es,rv}$	0.02	R_{pvb}	0.02	R_{pvb}	0.01
$E_{max,rv}$	0.07	$E_{shift,ra}$	0.07	$\tau_{es,rv}$	0.03	C_{sa}	0.01	C_{sa}	0.02	$E_{min,la}$	0.01
C_{pa}	0.07	$E_{min,rv}$	0.07	$E_{min,rv}$	0.03	$E_{max,lv}$	0.01	$E_{max,lv}$	0.02	$E_{min,rv}$	0.01
R_{pvb}	0.04	$E_{max,la}$	0.06	$\tau_{ep,lv}$	0.02	C_{pv}	0.01	C_{pv}	0.01	$E_{max,la}$	0.01
$E_{max,ra}$	0.03	$E_{max,rv}$	0.05	$E_{max,la}$	0.02	$E_{shift,ra}$	0.01	$E_{min,rv}$	0.01	$E_{max,lv}$	0.01
R_{sv}	0.02	$\tau_{ep,lv}$	0.04			$E_{min,rv}$	0.01	$E_{shift,ra}$	0.01	C_{sa}	0.01
$E_{min,la}$	0.02	$E_{min,la}$	0.03							C_{pv}	0.01
		$E_{max,ra}$	0.02								

Measurement Sets											
2A		2B		2C		2D		3A		3B	
P	E	P	E	P	E	P	E	P	E	P	E
$\tau_{ep,lv}$	0.18	$\tau_{ep,lv}$	0.12	$E_{shift,la}$	0.11	$E_{shift,ra}$	0.16	$\tau_{ep,lv}$	0.12	$E_{min,lv}$	0.1
$E_{shift,la}$	0.06	$E_{shift,ra}$	0.1	$\tau_{ep,lv}$	0.1	$E_{shift,la}$	0.06	$E_{min,lv}$	0.09	$\tau_{ep,lv}$	0.08
$E_{min,lv}$	0.04	$E_{shift,la}$	0.06	$E_{min,lv}$	0.08	$E_{min,lv}$	0.05	$E_{shift,ra}$	0.08	R_{svb}	0.08
$E_{shift,ra}$	0.04	$E_{min,lv}$	0.05	$E_{shift,ra}$	0.06	$\tau_{ep,lv}$	0.04	$E_{shift,la}$	0.07	$E_{shift,ra}$	0.07
$\tau_{es,lv}$	0.03	$\tau_{es,rv}$	0.03	$E_{min,la}$	0.05	$E_{min,rv}$	0.03	$E_{min,la}$	0.04	$E_{shift,la}$	0.07
$E_{max,lv}$	0.02	$\tau_{es,lv}$	0.03	$E_{max,lv}$	0.03	$E_{min,la}$	0.03	$\tau_{es,lv}$	0.03	$\tau_{es,lv}$	0.07
$\tau_{es,rv}$	0.02	$\tau_{ep,rv}$	0.03	$\tau_{es,lv}$	0.02	$\tau_{ep,rv}$	0.03	$E_{max,lv}$	0.03	$E_{min,la}$	0.04
R_{svb}	0.02	$E_{max,lv}$	0.02	C_{sv}	0.02	C_{sv}	0.02	C_{sv}	0.02	$E_{max,lv}$	0.03
C_{sv}	0.02	C_{sv}	0.02	$\tau_{es,rv}$	0.02	$E_{min,ra}$	0.02	$E_{min,rv}$	0.02	C_{sv}	0.03
C_{pa}	0.01	R_{svb}	0.02	R_{svb}	0.02	$\tau_{es,rv}$	0.02	R_{svb}	0.02	$E_{min,rv}$	0.03
C_{sa}	0.01	$E_{max,rv}$	0.02	$E_{max,la}$	0.02	$E_{max,rv}$	0.02	$E_{max,rv}$	0.02	C_{sa}	0.03
$E_{min,la}$	0.01	C_{pa}	0.01	$E_{max,rv}$	0.02	$E_{max,lv}$	0.02	C_{pv}	0.02	C_{pv}	0.03
C_{pv}	0.01	$E_{min,rv}$	0.01	C_{pa}	0.02	R_{svb}	0.02	C_{sa}	0.02	$E_{max,rv}$	0.02
$E_{min,rv}$	0.01	C_{sa}	0.01	C_{sa}	0.02	$E_{max,ra}$	0.02	$\tau_{es,rv}$	0.02	$E_{max,la}$	0.02
		C_{pv}	0.01	C_{pv}	0.02	C_{pa}	0.01	C_{pa}	0.02	C_{pa}	0.02
		$E_{min,la}$	0.01	$E_{min,rv}$	0.02	$\tau_{es,lv}$	0.01	$E_{max,la}$	0.01	$\tau_{es,rv}$	0.02
				$\tau_{ep,rv}$	0.01	C_{pv}	0.01	$\tau_{ep,rv}$	0.01	$\tau_{ep,rv}$	0.01
				R_{pvb}	0.01	$E_{max,la}$	0.01	$E_{min,ra}$	0.01	$E_{min,ra}$	0.01
						C_{sa}	0.01	$E_{max,ra}$	0.01	$E_{max,ra}$	0.01

Measurement Sets							
4A		4B		4C		4D	
P	E	P	E	P	E	P	E
$E_{min,lv}$	0.09	$E_{min,lv}$	0.09	$E_{shift,ra}$	0.18	$E_{shift,ra}$	0.16
$E_{shift,ra}$	0.08	$E_{shift,ra}$	0.09	$E_{min,rv}$	0.05	$E_{min,lv}$	0.08
R_{svb}	0.07	R_{svb}	0.07	$E_{min,lv}$	0.05	$E_{min,rv}$	0.05
$\tau_{ep,lv}$	0.06	$\tau_{ep,lv}$	0.06	R_{svb}	0.04	R_{svb}	0.04
$E_{shift,la}$	0.06	$E_{shift,la}$	0.05	C_{sv}	0.03	$E_{shift,la}$	0.04
$E_{min,rv}$	0.04	$E_{min,rv}$	0.04	$E_{shift,la}$	0.03	C_{sv}	0.03
$\tau_{es,lv}$	0.03	C_{sv}	0.04	$E_{min,ra}$	0.03	$\tau_{ep,lv}$	0.03
$E_{min,la}$	0.03	$E_{min,la}$	0.03	$\tau_{ep,rv}$	0.03	$E_{min,la}$	0.03
C_{sv}	0.03	$\tau_{es,lv}$	0.03	$\tau_{ep,lv}$	0.02	$E_{min,ra}$	0.03
$E_{max,lv}$	0.03	$E_{max,lv}$	0.03	$E_{max,rv}$	0.02	$E_{max,rv}$	0.03
$\tau_{ep,rv}$	0.02	$\tau_{es,rv}$	0.03	$\tau_{es,rv}$	0.02	$E_{max,lv}$	0.02
$\tau_{es,rv}$	0.02	$\tau_{ep,rv}$	0.03	$E_{max,ra}$	0.02	$\tau_{ep,rv}$	0.02
$E_{max,rv}$	0.02	$E_{max,rv}$	0.02	$E_{min,la}$	0.02	$\tau_{es,rv}$	0.02
C_{sa}	0.02	C_{pv}	0.02	$E_{max,lv}$	0.01	C_{pv}	0.02
C_{pv}	0.01	C_{sa}	0.01	C_{pv}	0.01	$E_{max,ra}$	0.02
C_{pa}	0.01	C_{pa}	0.01	C_{pa}	0.01	$\tau_{es,lv}$	0.02
$E_{min,ra}$	0.01	R_{pvb}	0.01	$\tau_{es,lv}$	0.01	C_{sa}	0.02
$E_{max,la}$	0.01	$E_{min,ra}$	0.01	R_{pvb}	0.01	C_{pa}	0.02
$E_{max,ra}$	0.01	$E_{max,ra}$	0.01	C_{sa}	0.01	R_{pvb}	0.01
		$E_{max,la}$	0.01			$E_{max,la}$	0.01

Table 6: **Input parameter rankings for continuous measurements:** Averaging across all output space, we display the input parameter rankings and its respective influence value for increasing continuous measurements.

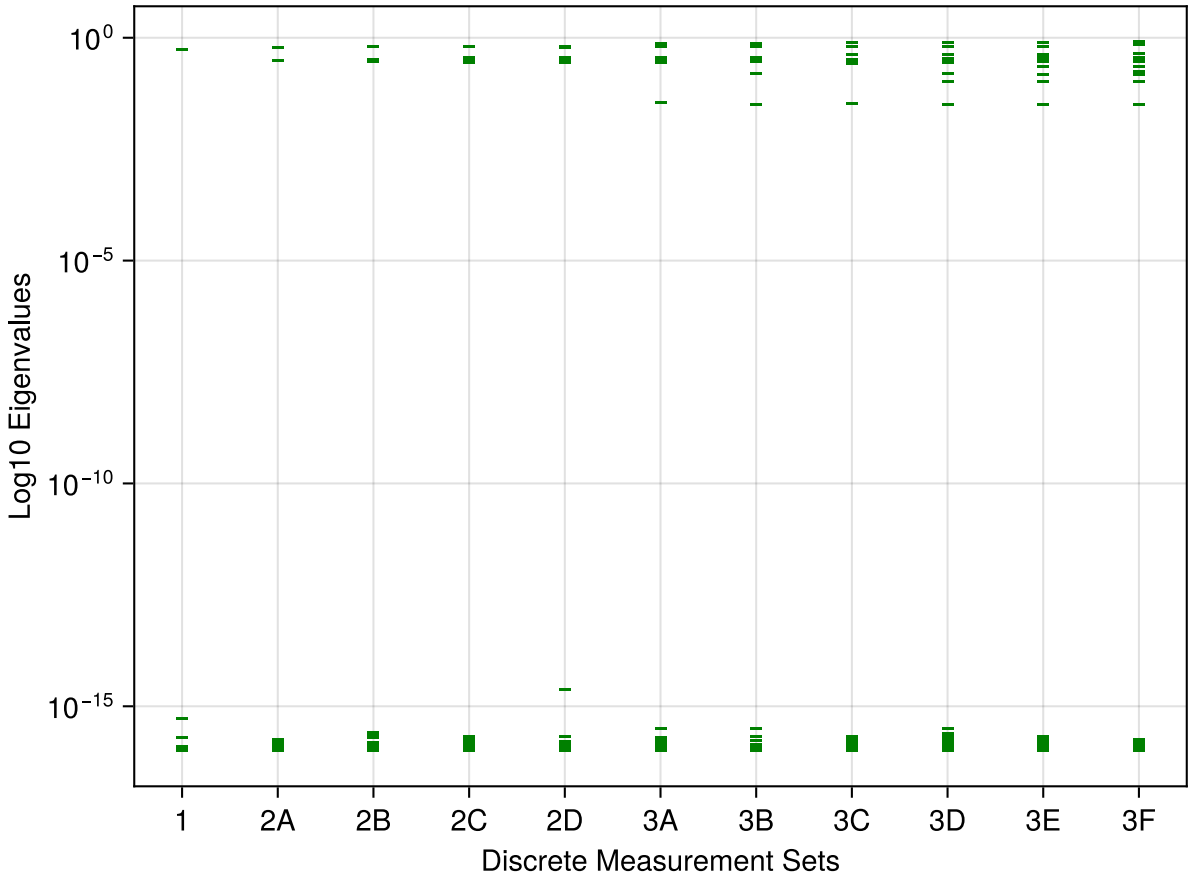

Figure 4: **Discrete measures - sloppy analysis:** The eigenvalues of the Fisher information matrix for increasing discrete measurements are displayed on a $\log_{10}$ scale.

9 in set 3D to 17 in set 4A. In set 7D which contains all discrete and continuous measurements, the exact same ranking as set 4D in table 6 displays, although the values of influence vary slightly. This indicates that continuous measurements dominate, when obtaining influential input parameters for a set of measurements. This pattern is also present in figure 6, where once continuous measurements are introduced to the output list, sloppiness appears and the eigenvalues are greater than 10^{0} with an eigen-spectrum ranging from 10^{-12} for set 4B decreasing down to 10^{-6} for set 7D. In sets 5A to 5D, the maximum flow in each chamber compartment was added to the optimisation process as a discrete measurement. Despite the number of discrete measurements outnumbering the number of continuous measurements, the addition of these discrete values had no influence on the ranking or sensitivity of the most influential parameters. It is important to note, however, that the maximum value of flow is contained in the continuous measurement so in affect no new information is provided to the solver, rather a weighting on the maxima of the flow is applied.

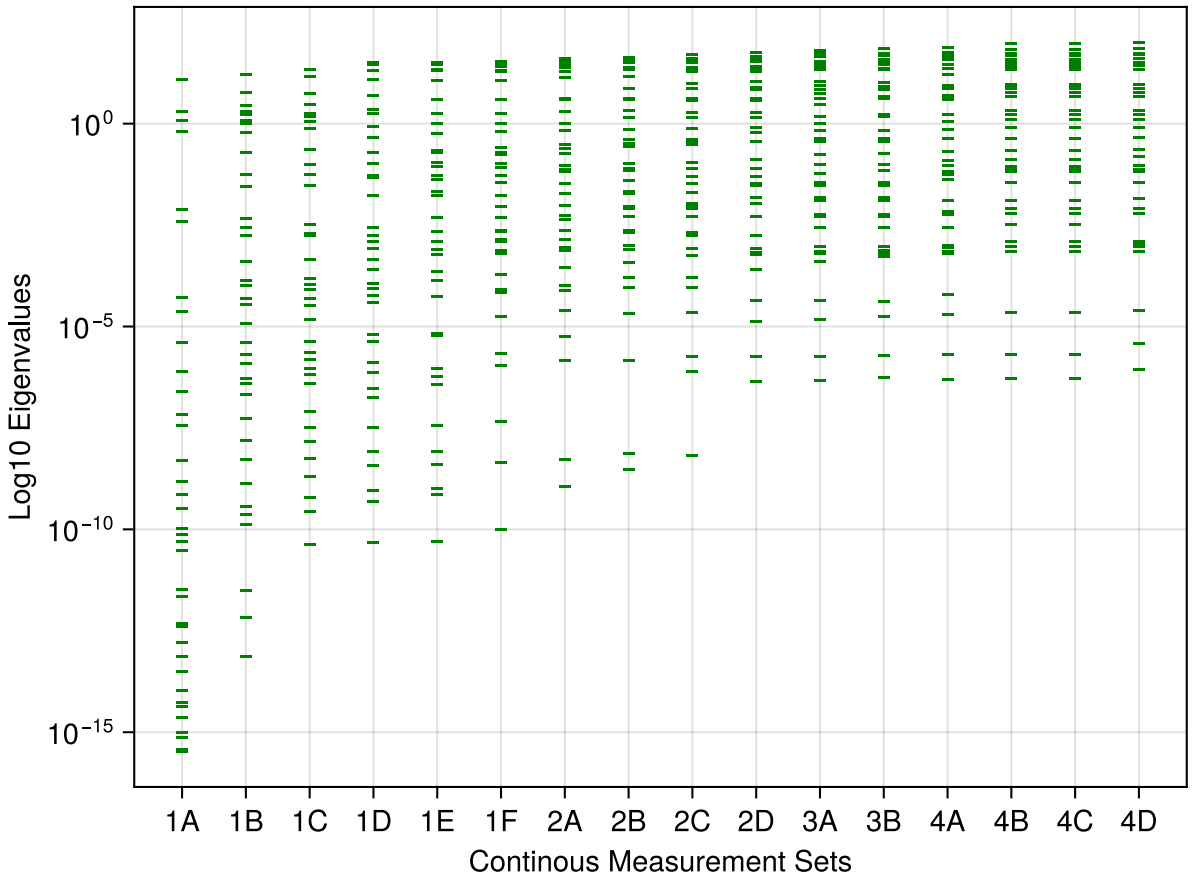

Figure 5: **Continuous measures - sloppy analysis:** The eigenvalues of the Fisher information matrix for increasing continuous measurements are displayed on a $\log_{10}$ scale.

Measurement Sets

1		2		3A		3B		3C		3D		4A		4B		4C		4D		4E		4F		5A	
P	E	P	E	P	E	P	E	P	E	P	E	P	E	P	E	P	E	P	E	P	E	P	E	P	E
C_{sa}	0.22	C_{sa}	0.80	C_{sa}	0.44	R_{svb}	0.34	R_{svb}	0.26	$E_{shift,ra}$	0.24	$E_{min,lv}$	0.44	$E_{min,lv}$	0.27	$\tau_{es,lv}$	0.38	$\tau_{ep,lv}$	0.25	$\tau_{ep,lv}$	0.20	$\tau_{ep,lv}$	0.11	$\tau_{ep,lv}$	0.1
R_{svb}	0.21	R_{svb}	0.60	R_{svb}	0.43	C_{sa}	0.33	C_{sa}	0.26	R_{svb}	0.10	R_{svb}	0.29	C_{pa}	0.16	$E_{min,lv}$	0.11	$E_{shift,la}$	0.16	$E_{shift,la}$	0.14	$E_{shift,la}$	0.09	$E_{shift,la}$	0.09
$\tau_{es,lv}$	0.17	$\tau_{es,lv}$	0.04	$E_{max,lv}$	0.24	$E_{max,lv}$	0.18	$E_{max,lv}$	0.14	C_{sa}	0.10	C_{sa}	0.23	R_{svb}	0.16	R_{svb}	0.09	$E_{min,lv}$	0.06	$\tau_{es,rv}$	0.05	$E_{shift,ra}$	0.09	$E_{shift,ra}$	0.09
				$V_{0,lv}$	0.04	$V_{0,lv}$	0.03	$V_{0,lv}$	0.03	$E_{max,lv}$	0.06	C_{sv}	0.22	$E_{shift,la}$	0.16	C_{sv}	0.06	$\tau_{es,lv}$	0.05	$E_{min,lv}$	0.05	$\tau_{es,rv}$	0.05	$\tau_{es,rv}$	0.05
				$\tau_{es,lv}$	0.02	$E_{max,rv}$	0.02	$E_{max,rv}$	0.02	$E_{max,ra}$	0.04	$\tau_{es,lv}$	0.17	C_{sv}	0.14	$E_{max,lv}$	0.06	C_{pa}	0.03	$\tau_{es,lv}$	0.04	$E_{min,lv}$	0.04	$E_{min,lv}$	0.04
						$\tau_{es,lv}$	0.02	$\tau_{es,lv}$	0.02	$\tau_{ep,rv}$	0.02	$E_{shift,ra}$	0.13	$\tau_{es,rv}$	0.12	C_{sa}	0.05	R_{svb}	0.02	C_{pa}	0.03	$\tau_{ep,rv}$	0.03	$\tau_{ep,rv}$	0.03
										$E_{min,rv}$	0.02	$E_{max,lv}$	0.13	R_{pvb}	0.11	$E_{shift,la}$	0.05	C_{sv}	0.02	R_{svb}	0.02	$\tau_{es,lv}$	0.03	$\tau_{es,lv}$	0.03
										$E_{max,rv}$	0.01	$E_{min,rv}$	0.12	C_{sa}	0.10	C_{pa}	0.04	$E_{min,la}$	0.02	C_{sv}	0.02	C_{pa}	0.02	C_{pa}	0.02
										$V_{0,lv}$	0.01	C_{pv}	0.11	$E_{shift,ra}$	0.09	$E_{shift,ra}$	0.03	$\tau_{es,rv}$	0.02	$E_{min,la}$	0.02	R_{svb}	0.02	R_{svb}	0.02
												$E_{shift,la}$	0.10	$E_{max,lv}$	0.08	$E_{min,rv}$	0.03	R_{pvb}	0.02	R_{pvb}	0.02	C_{sv}	0.02	C_{sv}	0.02
												$E_{max,rv}$	0.08	$E_{min,rv}$	0.08	C_{pv}	0.03	$E_{max,la}$	0.02	$E_{max,la}$	0.01	$E_{min,rv}$	0.01	$E_{min,rv}$	0.01
												$E_{max,la}$	0.06	C_{pv}	0.08	R_{pvb}	0.03	$E_{max,lv}$	0.01	$E_{max,lv}$	0.01	R_{pvb}	0.01	R_{pvb}	0.01
												$E_{max,ra}$	0.04	$\tau_{es,lv}$	0.07	$\tau_{es,rv}$	0.03	$E_{shift,ra}$	0.01	$E_{min,rv}$	0.01	$E_{min,la}$	0.01	$E_{min,la}$	0.01
												R_{sv}	0.04	$E_{max,rv}$	0.05	$E_{max,rv}$	0.02	$E_{min,rv}$	0.01	$E_{shift,ra}$	0.01	$E_{max,lv}$	0.01	$E_{max,lv}$	0.01
												C_{pa}	0.03	$E_{max,la}$	0.04	$E_{max,la}$	0.02	C_{sa}	0.01	C_{sa}	0.01	$E_{max,la}$	0.01	$E_{max,la}$	0.01
												R_{pvb}	0.03	$\tau_{ep,lv}$	0.04	$\tau_{ep,lv}$	0.01	C_{pv}	0.01	C_{pv}	0.01				
												$E_{min,la}$	0.01	$E_{max,ra}$	0.03	$E_{max,ra}$	0.01								
														R_{sv}	0.03	R_{sv}	0.01								
														$E_{min,la}$	0.03										

All input parameters register $E > 0.01$

Measurement Sets

5B		5C		5D		5E		5F		5G		5H		6A		6B		7A		7B		7C		7D	
P	E	P	E	P	E	P	E	P	E	P	E	P	E	P	E	P	E	P	E	P	E	P	E	P	
$\tau_{ep,lv}$	0.11	$\tau_{ep,lv}$	0.11	$\tau_{ep,lv}$	0.11	$\tau_{ep,lv}$	0.17	$\tau_{ep,lv}$	0.11	$E_{shift,la}$	0.11	$E_{shift,ra}$	0.16	$\tau_{ep,lv}$	0.12	$E_{min,lv}$	0.10	$E_{min,lv}$	0.09	$E_{min,lv}$	0.09	$E_{shift,ra}$	0.18	$E_{shift,ra}$	
$E_{shift,la}$	0.09	$E_{shift,la}$	0.09	$E_{shift,la}$	0.09	$E_{shift,la}$	0.06	$E_{shift,ra}$	0.10	$\tau_{ep,lv}$	0.09	$E_{shift,la}$	0.06	$E_{min,lv}$	0.09	$\tau_{ep,lv}$	0.08	$E_{shift,ra}$	0.09	$E_{shift,ra}$	0.09	$E_{min,rv}$	0.05	$E_{min,lv}$	
$E_{shift,ra}$	0.09	$E_{shift,ra}$	0.09	$E_{shift,ra}$	0.09	$E_{min,lv}$	0.05	$E_{shift,la}$	0.06	$E_{min,lv}$	0.07	$E_{min,lv}$	0.05	$E_{shift,ra}$	0.08	R_{svb}	0.08	R_{svb}	0.07	R_{svb}	0.07	$E_{min,lv}$	0.05	$E_{min,rv}$	
$\tau_{es,rv}$	0.05	$\tau_{es,rv}$	0.05	$\tau_{es,rv}$	0.05	$E_{shift,ra}$	0.04	$E_{min,lv}$	0.05	$E_{shift,ra}$	0.06	$\tau_{ep,lv}$	0.04	$E_{shift,la}$	0.07	$E_{shift,ra}$	0.07	$\tau_{ep,lv}$	0.06	$\tau_{ep,lv}$	0.05	R_{svb}	0.04	R_{svb}	
$E_{min,lv}$	0.04	$E_{min,lv}$	0.04	$E_{min,lv}$	0.04	$\tau_{es,lv}$	0.03	$\tau_{es,rv}$	0.03	$E_{min,la}$	0.05	$E_{min,rv}$	0.03	$E_{min,la}$	0.04	$E_{shift,la}$	0.06	$E_{shift,la}$	0.06	$E_{shift,la}$	0.05	C_{sv}	0.03	$E_{shift,la}$	
$\tau_{ep,rv}$	0.03	$\tau_{ep,rv}$	0.03	$\tau_{ep,rv}$	0.03	$E_{max,lv}$	0.02	$\tau_{ep,rv}$	0.03	$E_{max,lv}$	0.03	$E_{min,la}$	0.03	$\tau_{es,lv}$	0.03	$\tau_{es,lv}$	0.04	$E_{min,rv}$	0.04	$E_{min,rv}$	0.04	$E_{min,ra}$	0.03	C_{sv}	
$\tau_{es,lv}$	0.03	$\tau_{es,lv}$	0.03	$\tau_{es,lv}$	0.03	$\tau_{es,rv}$	0.02	$\tau_{es,lv}$	0.03	$\tau_{es,lv}$	0.03	$\tau_{ep,rv}$	0.03	C_{sv}	0.02	$E_{min,la}$	0.03	$\tau_{es,lv}$	0.03	C_{sv}	0.03	$E_{shift,la}$	0.03	$\tau_{ep,lv}$	
C_{pa}	0.02	C_{pa}	0.02	C_{pa}	0.02	R_{svb}	0.02	$E_{max,lv}$	0.02	C_{sv}	0.02	C_{sv}	0.03	$E_{max,lv}$	0.03	$E_{max,lv}$	0.03	$E_{min,la}$	0.03	$E_{min,la}$	0.03	$\tau_{ep,rv}$	0.02	$E_{min,la}$	
R_{svb}	0.02	R_{svb}	0.02	R_{svb}	0.02	C_{sv}	0.02	R_{svb}	0.02	$\tau_{es,rv}$	0.02	$E_{min,ra}$	0.02	C_{sv}	0.02	C_{sv}	0.03	$E_{max,lv}$	0.03	$\tau_{es,lv}$	0.03	$\tau_{es,lv}$	0.02	$E_{min,ra}$	
C_{sv}	0.02	C_{sv}	0.02	C_{sv}	0.02	C_{pa}	0.01	C_{sv}	0.02	R_{svb}	0.02	$\tau_{es,rv}$	0.02	$E_{min,rv}$	0.02	$E_{min,rv}$	0.02	C_{sv}	0.03	$E_{max,lv}$	0.03	$E_{max,rv}$	0.02	$E_{max,rv}$	
$E_{min,rv}$	0.01	$E_{min,rv}$	0.01	$E_{min,rv}$	0.01	C_{sa}	0.01	$E_{max,rv}$	0.02	$E_{max,la}$	0.02	$E_{max,rv}$	0.02	R_{svb}	0.02	$E_{max,rv}$	0.02	$E_{min,rv}$	0.02	$\tau_{ep,rv}$	0.02	$\tau_{es,rv}$	0.02	$E_{max,lv}$	
R_{pvb}	0.01	R_{pvb}	0.01	R_{pvb}	0.01	$E_{min,la}$	0.01	C_{pa}	0.02	$E_{max,rv}$	0.02	$E_{max,lv}$	0.02	C_{sa}	0.02	C_{sa}	0.02	$\tau_{es,rv}$	0.02	$\tau_{es,rv}$	0.02	$E_{max,ra}$	0.02	$\tau_{ep,rv}$	
$E_{min,la}$	0.01	$E_{min,la}$	0.01	$E_{min,la}$	0.01	C_{pv}	0.01	$E_{min,rv}$	0.02	C_{pa}	0.02	R_{svb}	0.02	C_{pv}	0.02	$E_{max,rv}$	0.02	$\tau_{ep,rv}$	0.02	$E_{max,rv}$	0.02	$E_{min,la}$	0.02	$\tau_{es,rv}$	
$E_{max,lv}$	0.01	$E_{max,lv}$	0.01	$E_{max,lv}$	0.01	$E_{min,rv}$	0.01	C_{sa}	0.01	C_{sa}	0.02	$E_{max,ra}$	0.02	C_{pv}	0.02	$E_{max,la}$	0.02	C_{sa}	0.02	C_{pv}	0.02	$E_{max,lv}$	0.02	C_{pv}	
$E_{max,la}$	0.01	$E_{max,la}$	0.01	$E_{max,la}$	0.01			C_{pv}	0.01	C_{pv}	0.02	$\tau_{es,lv}$	0.02	$E_{max,la}$	0.01	$\tau_{es,rv}$	0.01	C_{pa}	0.02	C_{sa}	0.02	C_{pv}	0.01	$E_{max,ra}$	
								$E_{min,la}$	0.01	$E_{min,rv}$	0.01	C_{pa}	0.02	C_{pa}	0.01	C_{pa}	0.01	C_{pa}	0.02	C_{pa}	0.02	C_{pa}	0.01	$\tau_{es,lv}$	
										$\tau_{ep,rv}$	0.01	C_{pv}	0.01	$\tau_{ep,rv}$	0.01	$E_{min,ra}$	0.01	$E_{min,ra}$	0.02	R_{pvb}	0.02	$\tau_{es,lv}$	0.01	C_{sa}	
										R_{pvb}	0.01	$E_{max,la}$	0.01	$E_{min,ra}$	0.01	$\tau_{ep,rv}$	0.01	$E_{max,ra}$	0.01	$E_{min,ra}$	0.02	R_{pvb}	0.01	C_{pa}	
												C_{sa}	0.01	$E_{max,ra}$	0.01	$E_{max,ra}$	0.01	$E_{max,ra}$	0.01	$E_{max,ra}$	0.01	C_{sa}	0.01	R_{pvb}	
																				$E_{max,ra}$	0.01			$E_{max,ra}$	

Table 7: **Input parameter ranking for mixed measurements:** The input parameter ranking and its respective influence value, averaging across all outputs, for increasing mixed measurements.

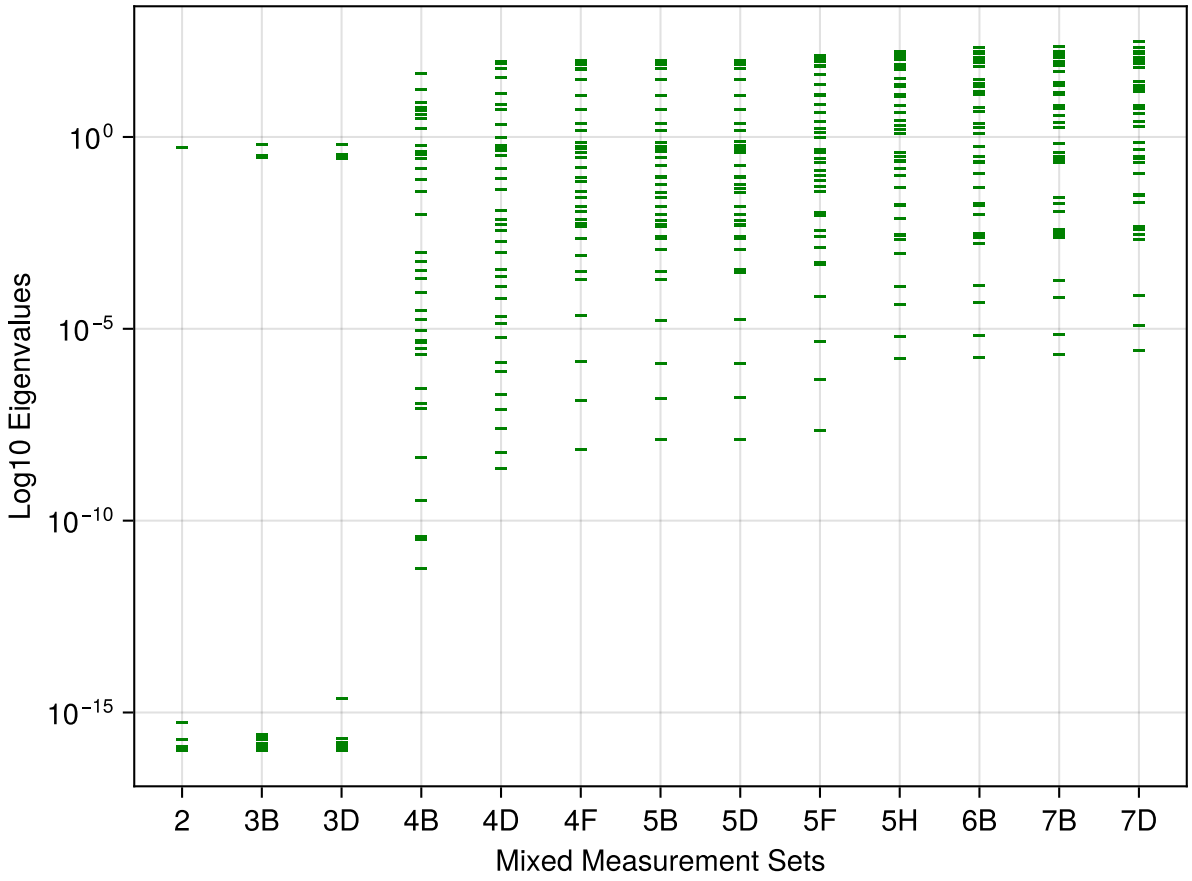

Figure 6: **Mixed measures - sloppy analysis:** The eigenvalues of the Fisher information matrix for every other increasing mixed measurements are displayed on a $\log_{10}$ scale.

5 Discussion

Our study aims to assess the impact of experimental design on the input parameter influence and the system sloppiness. Overall, the results largely agree with previous work: continuous measurements lead to a larger selected subset of input parameters as prime candidates for personalisation in a cardiovascular DT [53, 43, 56]. When only discrete measurements are used, there is a smaller and more concentrated subset of identifiable input parameters. Perhaps surprising is the quantitative extent of this disparity. Only when the largest discrete measurement set, 3F, is examined, we obtain the same number of input parameters with a value greater than 0.01, compared to the first continuous measurement set 1A.

We also observe that as the size of the output set increases, the influence between input parameters appears to become more evenly distributed. For example, for the discrete measurements results shown in table 5, the systemic vascular bed resistance R_{svb} and arterial compliance C_{sa} rank as the most influential parameters for all measurement sets except 2D. In set 1, C_{sa} and R_{svb} have influence values of 0.8 and 0.6 respectively. However, in set 3F, when the dimensionality of output space increases to 11, these two parameters' influence values decrease to 0.11 and 0.13.

The first sloppy analysis of this cardiovascular model indicates that discrete measurements do not introduce sloppiness into the system, whereas for continuous measurements, the system begins to exhibit sloppy behaviour. Through the perspective of creating DTs, the stiff input parameters are clearly identified using discrete measurements which would lead to easier identification of a personalised global minimum parameter set. When using the combination of both the continuous and discrete measurement sets, as they increase in size, the number of stiff input parameters which can be considered as prime candidates for personalisation increases. Sloppiness provides a view into the structure

of the input parameter space and an insight for why more “influential" input parameters appear when the dimensionality of the output grows. As more measurements are added, there is a noticeable change in the structure of the response surface, providing more guidance towards the personalisable global minimum. It should be noted that as more and more continuous signals are added, more outputs of the model are constrained. Therefore the increasing number of equally significant parameters is unsurprising. For specific use cases, this suggests that, where multiple data are available, a weighting of the most important clinical features may be required in the optimisation function to identify the required biomarkers.

When creating a virtual representation of a patient, it is still an open question whether the DT should be personalised to a specific condition or encapsulate the full physiological envelope of a patient [21, 8, 2]. Our experiments and analysis provides an insight to this question: if one wishes to capture a full physiological envelope through the DT, a number of continuous measurements are essential. This is due to the larger number of influential input parameters, along with the higher values of stiff eigenvalues, when compared to the discrete measurement setting. This approach brings practical problems of course, because of the invasive nature associated with obtaining some continuous measurements (for example, ventricular pressure). A patient would have to be subject to a series of invasive tests with associated risks, in order to generate the data to for a personalised DT. Alongside this, continuous measurements have shown a higher set of sloppiness, indicating that a computationally expensive optimisation routine may have to be utilised to generate the virtual patient representation. Conversely, if the purpose of a DT is to target specific conditions, a set of non-invasive discrete measurements poses as an alternative. Although there is a smaller number of identifiable input parameters in this case, the influence is concentrated strongly around the biomarkers relevant to the discrete metrics. In addition, because the system does not exhibit sloppy behaviour, the personalisation process using discrete measurements may be more efficient than its continuous counterparts. Additionally, continuous measurements taken clinically are also susceptible to noise from several sources, including equipment accuracy and differences in method between operators. In the case of time series data, noise can be present at varying sets at each time step, and therefore it is expected that noise in continuous data will have an increased effect on model sloppiness and parameter identifiability.

One problem of the sloppy analysis is the subjectivity in diagnosing whether sloppiness is present within a system. In this work, we have used the common definition of evenly spaced eigenvalues on a log scale, distributed over a minimum range of 10^6 orders of magnitude [59, 61]. The lack of sloppiness is clear in the discrete measurements setting (see figure 4). In the case of continuous measurements, when the measurement set increases, the distribution of eigenvalues (figure 5), while still evenly spaced, reduces from a spread of 10^{16} to just 10^6 (i.e., more input parameters are in the stiff direction than before). But does this change in an apparent reduction in sloppiness actually align with intuition? Given the increase of parameters in the stiff direction, one would assume more accurate optimisation of the input parameters when compared to set 1. However, this remains an open question and requires an additional study to investigate.

The study of sloppiness is common practice in most other areas of systems biology, however, this is not the case for cardiovascular models. The concept of sloppiness provides an important insight for examining the personalisability of cardiovascular models. By assessing the stiff and sloppy directions generated from the input parameters, sloppy analysis provides an alternative approach to identify optimal subsets for personalisation, compared to other methods such as profile likelihood and combining sensitivity and orthogonality [83, 56, 77]. This is an interesting area which should be explored in future research. When attempting to personalise a DT, there are several stages and sloppy analysis belongs to the vital off-line stage in which prime candidates for personalisation are identified. This off-line stage enables us to identify biomarkers for which can be personalised to produce the virtual representation of a patient. The off-line stage is vital because once patient data are introduced, any additional issues occurring during personalisation can then be attributed to issues within the clinical data. If we examine the parameters in figures 4-6 we observe that the rankings obtained by the analysing their influence (tables 5-7) are the same rankings obtained through the sloppy analysis. So in the discrete setting the systemic vascular bed resistance R_{svb} and the arterial compliance C_{sa} exhibit the largest eigenvalues making them the stiffest parameters in that setting. Thus these parameters are prime candidates for personlisation.

For the personalisation of cardiovascular DTs, the process in which this happens must operate on a multi-dimensional input parameter space in which some points give accurate representation of a patient’s physiological and pathophysiological state. Currently, much analysis on the input parameter space and the identification of the optimal parameter subset for personalisation are conducted on a local basis [23, 84, 85]. For example, it is still the norm to form the sensitivity matrices through local methods when analysing system sloppiness [34, 33]. If sloppy analysis is to be utilised more in the identification of biomarkers, local analysis should not be adopted for larger, more complex circulatory models. Personalisation is a global process, therefore it is vital to understand and quantify the global behaviour and the structure present within the input parameter space. This is why we have conducted our sloppiness analysis using the global sensitivity analysis outcomes in this work.

In order to perform such an extensive study, the associated computational expense is another important factor to consider. In total, we have tested 48 individual experimental designs, for each of which a sensitivity analysis has been performed with 75,000 samples to ensure convergence [73]. As our chosen global sensitivity method is Sobol indices [77, 23, 51], this means for each experimental design, $75000 \times (36 + 2) = 2.85 \times 10^6$ model evaluations are required. Thus for 48 independent experimental designs, we have solved the 4-chamber model 136.8 million times. This study has only been made feasible due to the superior computational speed exhibited by DifferentialEquations.jl within Julia in solving the dynamical system for a single model run including 30 cycles took 0.060246(s). When personalising DTs, computationally efficient and accurate tools should be utilised where possible, for the most effective allocation of computational resources for all stages of DT development. Of further interest in the development of LPMs in clinical use is the ability to validate the results of the model. Validation must be suitable for the context of use [86], and therefore also plays a key factor in experimental design, defining the clinical measurements taken and the choice of model output. Experimental design is therefore constricted not only by model behaviour as analysed here, but by clinical requirements. The requirement for testing in the context of use is one of the limitations of general cardiovascular models, as each use case must be included in the validation.

Alongside LPMs, there is also extensive research in higher dimensional (e.g. 1D, 2D and 3D) cardiovascular models which can be utilised as DTs [7, 87, 88]. The set of physiological details in these models is usually far superior to what can be established in LPMs. The main drawback or compromise, is the lack of ability to simulate global haemodynamics because of the astronomical computational cost. If we were able to create a full cardiovascular circulation representation, which could adapt to pathophysiological states, we would then be able to observe and predict other circulatory diseases, on top of the one in which the current condition occurs. Physiologically detailed models of a single piece of vessel or a compartment are of course of great importance, to further biological understanding where invasive clinical assessments are inappropriate or unethical. One promising area of the cardiovascular digital twin development is in the creation of multi-scale, multi-modal models, combining both LPMs and physiologically detailed higher dimensional representations of specific vessels or valves [44, 89]. This approach combines the advantages of both modelling domains and forms an attractive avenue for future research in cardiovascular personalisation and building DTs.

6 Conclusion

Our study highlights the importance of the experimental design for the quantification of input parameter influence and the associated sloppiness, for a lumped parameter personalised cardiovascular digital twin. Using a realistic 4-chamber 36-parameter LPM as a test bench, we investigated 48 independent experimental designs. The most significant findings, corresponding to the ones identified in Section 2.3, are: (i) Input parameter identifiability is not consistent when subject to varied measurement data and depends on the chosen experimental design. (ii) Sloppiness is present in LPMs, when the chosen experimental design contains continuous measurements. (iii) The personalisation of a digital twin to encompass a person's complete physiological envelope necessitates invasive tests to obtain continuous measurements. Although this approach offers an increased number of identifiable parameters with potentials to be biomarkers, it comes at the expense of a sloppy system which in turn increases the difficulty in parameter identification. Conversely, discrete metrics may provide a simpler personalisation approach, yielding less identifiable but more targeted biomarkers, due to the absence of sloppiness in the system.

Acknowledgements

CVD-Net, We gratefully acknowledge Polish high-performance computing infrastructure PLGrid (HPC Center: ACK Cyfronet AGH) for providing computer facilities and support within computational grant no. PLG/2024/017108.

Author Contributions

Conceptualisation: H.S, I.H, X.X, D.T; Formal Analysis: H.S, X.X; Methodology: H.S, X.X, I.H, T.S, D.T, T.N; Visulisation: H.S, G.F; Software: H.S, T.S; Supervision: I.H, X.X, R.C, T.S; Validation: X.X, I.H; Funding Acquisition: X.X, I.H, T.S; Writing – Original Draft Preparation: H.S, X.X, I.H, D.T; Writing – Review & Editing: X.X, I.H, G.F, R.C, T.S, P.M.

Conflict of interest

The authors declare no conflict of interest.

Data Availability Statement

All code used to generate the findings in this study can be found at the Github link `https://github.com/H-Sax/Measurements`.

References

[1] AIAA Digital Engineering Integration Committee et al. Digital twin: Definition & value—an aiaa and aia position paper. *AIAA: Reston, VA, USA*, 2020.

[2] Natalia A Trayanova and Adityo Prakosa. Up digital and personal: How heart digital twins can transform heart patient care. *Heart Rhythm*, 21(1):89–99, 2024.

[3] Karli Gillette, Matthias AF Gsell, Anton J Prassl, Elias Karabelas, Ursula Reiter, Gert Reiter, Thomas Grandits, Christian Payer, Darko Štern, Martin Urschler, et al. A framework for the generation of digital twins of cardiac electrophysiology from clinical 12-leads ecgs. *Medical Image Analysis*, 71:102080, 2021.

[4] Genevieve Coorey, Gemma A Figtree, David F Fletcher, Victoria J Snelson, Stephen Thomas Vernon, David Winlaw, Stuart M Grieve, Alistair McEwan, Jean Yee Hwa Yang, Pierre Qian, et al. The health digital twin to tackle cardiovascular disease—a review of an emerging interdisciplinary field. *NPJ digital medicine*, 5(1):126, 2022.

[5] Francesco Viola, Giulio Del Corso, Ruggero De Paulis, and Roberto Verzicco. Gpu accelerated digital twins of the human heart open new routes for cardiovascular research. *Scientific reports*, 13(1):8230, 2023.

[6] Erin P Balogh, Bryan T Miller, John R Ball, and National Academies of Sciences. Technology and tools in the diagnostic process, 2015.

[7] Steven A Niederer, Joost Lumens, and Natalia A Trayanova. Computational models in cardiology. *Nature Reviews Cardiology*, 16(2):100–111, 2019.

[8] D Rodney Hose, Patricia V Lawford, Wouter Huberts, Leif Rune Hellevik, Stig W Omholt, and Frans N van de Vosse. Cardiovascular models for personalised medicine: Where now and where next? *Medical engineering & physics*, 72:38–48, 2019.

[9] Yubing Shi, Patricia Lawford, and Rodney Hose. Review of zero-d and 1-d models of blood flow in the cardiovascular system. *Biomedical engineering online*, 10:1–38, 2011.

[10] Nico Westerhof, Jan-Willem Lankhaar, and Berend E Westerhof. The arterial windkessel. *Medical & biological engineering & computing*, 47(2):131–141, 2009.

[11] Nicolaas Westerhof, Nikolaos Stergiopulos, Mark IM Noble, and Berend E Westerhof. *Snapshots of hemodynamics: an aid for clinical research and graduate education*. Springer, 2018.

[12] Jorge Corral-Acero, Francesca Margara, Maciej Marciniak, Cristobal Rodero, Filip Loncaric, Yingjing Feng, Andrew Gilbert, Joao F Fernandes, Hassaan A Bukhari, Ali Wajdan, et al. The 'digital twin'to enable the vision of precision cardiology. *European heart journal*, 41(48):4556–4564, 2020.

[13] Sean P Murphy, Nasrien E Ibrahim, and James L Januzzi. Heart failure with reduced ejection fraction: a review. *Jama*, 324(5):488–504, 2020.

[14] Anthony M Dart and Bronwyn A Kingwell. Pulse pressure—a review of mechanisms and clinical relevance. *Journal of the American College of Cardiology*, 37(4):975–984, 2001.

[15] Peter D Gatehouse, Jennifer Keegan, Lindsey A Crowe, Sharmeen Masood, Raad H Mohiaddin, Karl-Friedrich Kreitner, and David N Firmin. Applications of phase-contrast flow and velocity imaging in cardiovascular mri. *European radiology*, 15:2172–2184, 2005.

[16] Jamal A Alhashemi, Maurizio Cecconi, and Christoph K Hofer. Cardiac output monitoring: an integrative perspective. *Critical Care*, 15(2):214, 2011.

[17] Kiichi Sagawa. The ventricular pressure-volume diagram revisited. *Circulation Research*, 43(5):677–687, 1978.

[18] Roger E Kirk. Experimental design. *Sage handbook of quantitative methods in psychology*, pages 23–45, 2009.

[19] Albert Tarantola. *Inverse problem theory and methods for model parameter estimation*. SIAM, 2005.

[20] Kyle Strimbu and Jorge A Tavel. What are biomarkers? *Current Opinion in HIV and AIDS*, 5(6):463, 2010.

[21] Wouter Huberts, Stefan GH Heinen, Niek Zonnebeld, Daniel AF van den Heuvel, Jean-Paul PM de Vries, Jan HM Tordoir, D Rodney Hose, Tammo Delhaas, and Frans N van de Vosse. What is needed to make cardiovascular models suitable for clinical decision support? a viewpoint paper. *Journal of computational science*, 24:68–84, 2018.

[22] Andrea Saltelli, Stefano Tarantola, Francesca Campolongo, Marco Ratto, et al. *Sensitivity analysis in practice: a guide to assessing scientific models*, volume 1. Wiley Online Library, 2004.

[23] Christian Haargaard Olsen, Johnny T Ottesen, Ralph C Smith, and Mette S Olufsen. Parameter subset selection techniques for problems in mathematical biology. *Biological cybernetics*, 113:121–138, 2019.

[24] Andrea Saltelli, Marco Ratto, Terry Andres, Francesca Campolongo, Jessica Cariboni, Debora Gatelli, Michaela Saisana, and Stefano Tarantola. *Global sensitivity analysis: the primer*. John Wiley & Sons, 2008.

[25] Ror Bellman and Karl Johan Åström. On structural identifiability. *Mathematical biosciences*, 7(3-4):329–339, 1970.

[26] Athanassios Iliadis. Structural identifiability and sensitivity. *Journal of pharmacokinetics and pharmacodynamics*, 46(2):127–135, 2019.

[27] Franz-Georg Wieland, Adrian L Hauber, Marcus Rosenblatt, Christian Tönsing, and Jens Timmer. On structural and practical identifiability. *Current Opinion in Systems Biology*, 25:60–69, 2021.

[28] Bryan C Daniels, Yan-Jiun Chen, James P Sethna, Ryan N Gutenkunst, and Christopher R Myers. Sloppiness, robustness, and evolvability in systems biology. *Current opinion in biotechnology*, 19(4):389–395, 2008.

[29] Lucian Mihai Itu, Puneet Sharma, and Constantin Suciu. *Patient-specific hemodynamic computations: application to personalized diagnosis of cardiovascular pathologies*. Springer, 2017.

[30] Mykel J Kochenderfer and Tim A Wheeler. *Algorithms for optimization*. Mit Press, 2019.

[31] Harry Saxton, Torsten Schenkel, Ian Halliday, and Xu Xu. Personalised parameter estimation of the cardiovascular system: Leveraging data assimilation and sensitivity analysis. *Journal of Computational Science*, 74:102158, 2023.

[32] Oana-Teodora Chis, Alejandro F Villaverde, Julio R Banga, and Eva Balsa-Canto. On the relationship between sloppiness and identifiability. *Mathematical biosciences*, 282:147–161, 2016.

[33] Ryan N Gutenkunst, Joshua J Waterfall, Fergal P Casey, Kevin S Brown, Christopher R Myers, and James P Sethna. Universally sloppy parameter sensitivities in systems biology models. *PLoS computational biology*, 3(10):e189, 2007.

[34] Gloria M Monsalve-Bravo, Brodie AJ Lawson, Christopher Drovandi, Kevin Burrage, Kevin S Brown, Christopher M Baker, Sarah A Vollert, Kerrie Mengersen, Eve McDonald-Madden, and Matthew P Adams. Analysis of sloppiness in model simulations: Unveiling parameter uncertainty when mathematical models are fitted to data. *Science advances*, 8(38):eabm5952, 2022.

[35] Jason Carson, Lynne Warrander, Edward Johnstone, and Raoul van Loon. Personalising cardiovascular network models in pregnancy: A two-tiered parameter estimation approach. *International Journal for Numerical Methods in Biomedical Engineering*, 37(11):e3267, 2021.

[36] Matteo Salvador, Fanwei Kong, Mathias Peirlinck, David Parker, Henry Chubb, Anne Dubin, and Alison Marsden. Digital twinning of cardiac electrophysiology for congenital heart disease. *Biorxiv*, pages 2023–11, 2023.

[37] Tobias Gerach, Steffen Schuler, Jonathan Fröhlich, Laura Lindner, Ekaterina Kovacheva, Robin Moss, Eike Moritz Wülfers, Gunnar Seemann, Christian Wieners, and Axel Loewe. Electro-mechanical whole-heart digital twins: a fully coupled multi-physics approach. *Mathematics*, 9(11):1247, 2021.

[38] TG Myers, Vicent Ribas Ripoll, Anna Sáez de Tejada Cuenca, Sarah L Mitchell, and Mark J McGuinness. Modelling the cardiovascular system for assessing the blood pressure curve. *Mathematics-in-industry case studies*, 8:1–16, 2017.

[39] Zheng Duanmu, Min Yin, Xueling Fan, Xilan Yang, and Xiaoyu Luo. A patient-specific lumped-parameter model of coronary circulation. *Scientific reports*, 8(1):874, 2018.

[40] Neeraj Kavan Chakshu, Igor Sazonov, and Perumal Nithiarasu. Towards enabling a cardiovascular digital twin for human systemic circulation using inverse analysis. *Biomechanics and modeling in mechanobiology*, 20(2):449–465, 2021.

[41] Daniel Canuto, Joe L Pantoja, Joyce Han, Erik P Dutson, and Jeff D Eldredge. An ensemble kalman filter approach to parameter estimation for patient-specific cardiovascular flow modeling. *Theoretical and Computational Fluid Dynamics*, 34:521–544, 2020.

[42] Sanjay Pant, Chiara Corsini, Catriona Baker, Tain-Yen Hsia, Giancarlo Pennati, Irene E Vignon-Clementel, Modeling of Congenital Hearts Alliance (MOCHA) Investigators, et al. Data assimilation and modelling of patient-specific single-ventricle physiology with and without valve regurgitation. *Journal of biomechanics*, 49(11):2162–2173, 2016.

[43] Amanda L Colunga, Mitchel J Colebank, REU Program, and Mette S Olufsen. Parameter inference in a computational model of haemodynamics in pulmonary hypertension. *Journal of the Royal Society Interface*, 20(200):20220735, 2023.

[44] Marina Strocchi, Stefano Longobardi, Christoph M Augustin, Matthias AF Gsell, Argyrios Petras, Christopher A Rinaldi, Edward J Vigmond, Gernot Plank, Chris J Oates, Richard D Wilkinson, et al. Cell to whole organ global sensitivity analysis on a four-chamber heart electromechanics model using gaussian processes emulators. *PLOS Computational Biology*, 19(6):e1011257, 2023.

[45] Friederike Schäfer, Jacob Sturdy, and Leif Rune Hellevik. Age and sex-dependent sensitivity analysis of a common carotid artery model. *Biomechanics and Modeling in Mechanobiology*, pages 1–19, 2024.

[46] Belén Casas, Jonas Lantz, Federica Viola, Gunnar Cedersund, Ann F Bolger, Carl-Johan Carlhäll, Matts Karlsson, and Tino Ebbers. Bridging the gap between measurements and modelling: a cardiovascular functional avatar. *Scientific reports*, 7(1):6214, 2017.

[47] Antoine Pironet, Pierre C Dauby, J Geoffrey Chase, Paul D Docherty, James A Revie, and Thomas Desaive. Structural identifiability analysis of a cardiovascular system model. *Medical engineering & physics*, 38(5):433–441, 2016.

[48] Antoine Pironet, Paul D Docherty, Pierre C Dauby, J Geoffrey Chase, and Thomas Desaive. Practical identifiability analysis of a minimal cardiovascular system model. *Computer methods and programs in biomedicine*, 171:53–65, 2019.

[49] Andrew D Marquis, Andrea Arnold, Caron Dean-Bernhoft, Brian E Carlson, and Mette S Olufsen. Practical identifiability and uncertainty quantification of a pulsatile cardiovascular model. *Mathematical biosciences*, 304:9–24, 2018.

[50] Sébastien de Bournonville, Antoine Pironet, Chris Pretty, J Geoffrey Chase, and Thomas Desaive. Parameter estimation in a minimal model of cardio-pulmonary interactions. *Mathematical Biosciences*, 313:81–94, 2019.

[51] Lorenzo Sala, Nicolas Golse, Alexandre Joosten, Eric Vibert, and Irene Vignon-Clementel. Sensitivity analysis of a mathematical model simulating the post-hepatectomy hemodynamics response. *Annals of Biomedical Engineering*, 51(1):270–289, 2023.

[52] Feng Huang and Shunv Ying. On-line parameter identification of the lumped arterial system model: A simulation study. *Plos one*, 15(7):e0236012, 2020.

[53] Nikolai L Bjørdalsbakke, Jacob T Sturdy, David R Hose, and Leif R Hellevik. Parameter estimation for closed-loop lumped parameter models of the systemic circulation using synthetic data. *Mathematical biosciences*, 343:108731, 2022.

[54] Christopher E Hann, J Geoffrey Chase, Thomas Desaive, CB Froissart, J Revie, D Stevenson, Bernard Lambermont, Alexandre Ghuysen, Philippe Kolh, and Geoffrey M Shaw. Unique parameter identification for cardiac diagnosis in critical care using minimal data sets. *Computer methods and programs in biomedicine*, 99(1):75–87, 2010.

[55] VG Eck, J Sturdy, and LR Hellevik. Effects of arterial wall models and measurement uncertainties on cardiovascular model predictions. *Journal of biomechanics*, 50:188–194, 2017.

[56] Mitchel J Colebank and Naomi C Chesler. An in-silico analysis of experimental designs to study ventricular function: A focus on the right ventricle. *PLoS computational biology*, 18(9):e1010017, 2022.

[57] Hannes Hettling and Johannes HGM van Beek. Analyzing the functional properties of the creatine kinase system with multiscale 'sloppy'modeling. *PLoS computational biology*, 7(8):e1002130, 2011.

[58] D Joubert, JD Stigter, and J Molenaar. Determining minimal output sets that ensure structural identifiability. *PLoS One*, 13(11):e0207334, 2018.

[59] Prem Jagadeesan, Karthik Raman, and Arun K Tangirala. Sloppiness: Fundamental study, new formalism and its application in model assessment. *Plos one*, 18(3):e0282609, 2023.

[60] Daniel Silk, Paul DW Kirk, Chris P Barnes, Tina Toni, and Michael PH Stumpf. Model selection in systems biology depends on experimental design. *PLoS computational biology*, 10(6):e1003650, 2014.

[61] Andrew White, Malachi Tolman, Howard D Thames, Hubert Rodney Withers, Kathy A Mason, and Mark K Transtrum. The limitations of model-based experimental design and parameter estimation in sloppy systems. *PLoS computational biology*, 12(12):e1005227, 2016.

[62] Joshua F Apgar, David K Witmer, Forest M White, and Bruce Tidor. Sloppy models, parameter uncertainty, and the role of experimental design. *Molecular BioSystems*, 6(10):1890–1900, 2010.

[63] Dominic G Whittaker, Jiahui Wang, Joseph G Shuttleworth, Ravichandra Venkateshappa, Jacob M Kemp, Thomas W Claydon, and Gary R Mirams. Ion channel model reduction using manifold boundaries. *Journal of the Royal Society Interface*, 19(193):20220193, 2022.

[64] Johannes HGM Van Beek, Anne-Christin Hauschild, Hannes Hettling, and Thomas W Binsl. Robust modelling, measurement and analysis of human and animal metabolic systems. *Philosophical Transactions of the Royal Society A: Mathematical, Physical and Engineering Sciences*, 367(1895):1971–1992, 2009.

[65] Dominic G Whittaker, Michael Clerx, Chon Lok Lei, David J Christini, and Gary R Mirams. Calibration of ionic and cellular cardiac electrophysiology models. *Wiley Interdisciplinary Reviews: Systems Biology and Medicine*, 12(4):e1482, 2020.

[66] Giulia Comunale, Paolo Peruzzo, Biagio Castaldi, Renato Razzolini, Giovanni Di Salvo, Massimo A Padalino, and Francesca M Susin. Understanding and recognition of the right ventricular function and dysfunction via a numerical study. *Scientific Reports*, 11(1):3709, 2021.

[67] Theodosios Korakianitis and Yubing Shi. Numerical simulation of cardiovascular dynamics with healthy and diseased heart valves. *Journal of biomechanics*, 39(11):1964–1982, 2006.

[68] Hiroyuki Suga and Kiichi Sagawa. Instantaneous pressure-volume relationships and their ratio in the excised, supported canine left ventricle. *Circulation research*, 35(1):117–126, 1974.

[69] Torsten Schenkel. Circulatory system models, December 2023.

[70] Gerhard Wanner and Ernst Hairer. *Solving ordinary differential equations II*, volume 375. Springer Berlin Heidelberg New York, 1996.

[71] Ilya M Sobol. Global sensitivity indices for nonlinear mathematical models and their monte carlo estimates. *Mathematics and computers in simulation*, 55(1-3):271–280, 2001.

[72] Michiel JW Jansen. Analysis of variance designs for model output. *Computer Physics Communications*, 117(1-2):35–43, 1999.

[73] Harry Saxton, Xu Xu, Torsten Schenkel, Richard H Clayton, and Ian Halliday. Convergence, sampling and total order estimator effects on parameter orthogonality in global sensitivity analysis. *bioRxiv*, pages 2024–02, 2024.

[74] GEB Archer, Andrea Saltelli, and Ilya Meyerovich Sobol. Sensitivity measures, anova-like techniques and the use of bootstrap. *Journal of Statistical Computation and Simulation*, 58(2):99–120, 1997.

[75] Ronald A Fisher. On the mathematical foundations of theoretical statistics. *Philosophical transactions of the Royal Society of London. Series A, containing papers of a mathematical or physical character*, 222(594-604):309–368, 1922.

[76] Yannis Pantazis, Markos A Katsoulakis, and Dionisios G Vlachos. Parametric sensitivity analysis for biochemical reaction networks based on pathwise information theory. *BMC bioinformatics*, 14:1–19, 2013.

[77] Harry Saxton, Xu Xu, Torsten Schenkel, and Ian Halliday. Assessing input parameter hyperspace and parameter identifiability in a cardiovascular system model via sensitivity analysis. *Journal of Computational Science*, 79:102287, 2024.

[78] Jiannan Yang. Decision-oriented two-parameter fisher information sensitivity using symplectic decomposition. *Technometrics*, 66(1):28–39, 2024.

[79] Rujun Li, Michael A Henson, and Michael J Kurtz. Selection of model parameters for off-line parameter estimation. *IEEE Transactions on control systems technology*, 12(3):402–412, 2004.

[80] Hervé Abdi and Lynne J Williams. Principal component analysis. *Wiley interdisciplinary reviews: computational statistics*, 2(4):433–459, 2010.

[81] Kevin S Brown and James P Sethna. Statistical mechanical approaches to models with many poorly known parameters. *Physical review E*, 68(2):021904, 2003.

[82] Joshua J Waterfall, Fergal P Casey, Ryan N Gutenkunst, Kevin S Brown, Christopher R Myers, Piet W Brouwer, Veit Elser, and James P Sethna. Sloppy-model universality class and the vandermonde matrix. *Physical review letters*, 97(15):150601, 2006.

[83] Clemens Kreutz, Andreas Raue, Daniel Kaschek, and Jens Timmer. Profile likelihood in systems biology. *The FEBS journal*, 280(11):2564–2571, 2013.

[84] Pablo J Blanco, Sansuke M Watanabe, Marco Aurélio RF Passos, Pedro A Lemos, and Raúl A Feijóo. An anatomically detailed arterial network model for one-dimensional computational hemodynamics. *IEEE Transactions on biomedical engineering*, 62(2):736–753, 2014.

[85] Lucas O Müller, Sansuke M Watanabe, Eleuterio F Toro, Raúl A Feijóo, and Pablo J Blanco. An anatomically detailed arterial-venous network model. cerebral and coronary circulation. *Frontiers in Physiology*, 14:1162391, 2023.

[86] Marco Viceconti, Francesco Pappalardo, Blanca Rodriguez, Marc Horner, Jeff Bischoff, and Flora Musuamba Tshinanu. In silico trials: Verification, validation and uncertainty quantification of predictive models used in the regulatory evaluation of biomedical products. *Methods*, 185:120–127, 1 2021.

[87] Daniel J Taylor, Jeroen Feher, Krzysztof Czechowicz, Ian Halliday, DR Hose, Rebecca Gosling, Louise Aubiniere-Robb, Marcel van't Veer, Danielle CJ Keulards, Pim Tonino, et al. Validation of a novel numerical model to predict regionalized blood flow in the coronary arteries. *European Heart Journal-Digital Health*, 4(2):81–89, 2023.

[88] Daniel J Taylor, Harry Saxton, Ian Halliday, Tom Newman, Jeroen Feher, Rebecca Gosling, Andrew J Narracott, Denise van Kemenade, Marcel van't Veer, Pim AL Tonino, et al. Evaluation of models of sequestration flow in coronary arteries—physiology versus anatomy? *Computers in Biology and Medicine*, 173:108299, 2024.

[89] Matteo Salvador, Marina Strocchi, Francesco Regazzoni, Christoph M Augustin, Luca Dede', Steven A Niederer, and Alfio Quarteroni. Whole-heart electromechanical simulations using latent neural ordinary differential equations. *NPJ Digital Medicine*, 7(1):90, 2024.